Journal of African Earth Sciences 57 (2010) 47–69

Contents lists available at ScienceDirect

Journal of African Earth Sciences

journal homepage: www.elsevier.com/locate/jafrearsci

Lithostratigraphy, biostratigraphy and chemostratigraphy of Upper Cretaceous sediments from southern Tanzania: Tanzania drilling project sites 21–26

Álvaro Jiménez Berrocoso [a,*], Kenneth G. MacLeod [a], Brian T. Huber [b], Jacqueline A. Lees [c], Ines Wendler [d], Paul R. Bown [c], Amina K. Mweneinda [e], Carolina Isaza Londoño [a], Joyce M. Singano [f]

[a] Department of Geological Sciences, University of Missouri, Columbia, MO 65211, USA
[b] Department of Paleobiology, MRC 121, Smithsonian Museum of Natural History, Washington, DC 20013-7012, USA
[c] Department of Earth Sciences, University College London, Gower Street, London WC1E 6BT, UK
[d] Universität Bremen, FB 5, Postfach 330 440, D-28334 Bremen, Germany
[e] School of Earth, Ocean and Planetary Sciences, Cardiff University, Park Place, Cardiff CF10 3YE, UK
[f] Tanzania Petroleum Development Corporation, P.O. Box 2774, Dar-es-Salaam, Tanzania

ARTICLE INFO

Article history:
Received 20 March 2009
Received in revised form 19 July 2009
Accepted 23 July 2009
Available online 6 August 2009

Keywords:
Tanzania drilling project
Late Cretaceous biostratigraphy
Clay-rich shelfal facies
Glassy foraminifera
Holococcoliths
OAE2 isotopic excursion

ABSTRACT

The 2007 drilling season by the Tanzania drilling project (TDP) reveals a much more expanded Upper Cretaceous sequence than was recognized previously in the Lindi region of southern Tanzania. This TDP expedition targeted recovery of excellently preserved microfossils (foraminifera and calcareous nannofossils) for Late Cretaceous paleoclimatic, paleoceanographic and biostratigraphic studies. A total of 501.17 m of core was drilled at six Upper Cretaceous sites (TDP Sites 21, 22, 23, 24, 24B and 26) and a thin Miocene–Pleistocene section (TDP Site 25). Microfossil preservation at all these sites is good to excellent, with foraminifera often showing glassy shells and consistently good preservation of small and delicate nannofossil taxa. In addition to adding to our knowledge of the subsurface geology, new surface exposures were mapped and the geological map of the region is revised herein.

TDP Sites 24, 24B and 26 collectively span the upper Albian to lower-middle Turonian (planktonic foraminiferal *Planomalina buxtorfi–Whiteinella archaeocretacea* Zones and calcareous nannofossil zones UC0a–UC8a). The bottom of TDP Site 21 is barren, but the rest of the section represents the uppermost Cenomanian–Coniacian (*W. archaeocretacea–Dicarinella concavata* Zones and nannofossil zones UC5c–UC10). Bulk organic $\delta^{13}C$ data suggest recovery of part of Ocean Anoxic Event 2 (OAE2) from these four sites. In the upper part of this interval, the lower Turonian nannofossil zones UC6a–7 are characterized by a low-diversity nannoflora that may be related to OAE2 surface-water conditions. TDP Site 22 presents a 122-m-thick, lower-middle Turonian (*W. archaeocretacea–Helvetoglobotruncana helvetica* Zones) sequence that includes the nannofossil zones UC6a(-7?), but invariable isotopic curves. Further, a lower to upper Campanian (*Globotruncana ventricosa–Radotruncana calcarata* Zones and nannofossil subzones $UC15b^{TP}$–$UC15d^{TP}$) succession was drilled at TDP Site 23. Lithologies of the new sites include thin units of gray, medium to coarse sandstones, separating much thicker intervals of dark claystones with organic-rich laminated parts, irregular silty to fine sandstone partings, and rare inoceramid and ammonite debris. These lithofacies are interpreted to have been deposited in outer shelf and upper slope settings and indicate relatively stable sedimentary conditions during most of the Late Cretaceous on the Tanzanian margin.

1. Introduction

The sediments of southern coastal Tanzania have been targeted in recent years by the Tanzania drilling project (TDP), an informal collaboration of researchers studying Upper Cretaceous–Neogene stratigraphy, micropaleontology and paleoclimate. TDP studies have recovered distinctly diverse assemblages of excellently preserved foraminifera (Pearson et al., 2001; Handley et al., 2008) and nannofossils (Bown, 2005; Bown and Dunkley Jones, 2006; Lees, 2007) from outcrop and core sediment samples. Also, stable isotope measurements on these samples have yielded reliable temperature estimates for the Miocene (Stewart et al., 2004), Eocene (Pearson et al., 2001, 2007, 2008) and Maastrichtian (Pearson et al., 2001). The excellent preservation of the microfossils seems

* Corresponding author. Present address: School of Earth, Atmospheric and Environmental Sciences, University of Manchester, Williamson Building, Oxford Road, Manchester M13 9PL, UK.
E-mail address: alvaro.jimenezberrocoso@manchester.ac.uk (Á. Jiménez Berrocoso).

1464-343X/$ - see front matter © 2009 Elsevier Ltd. All rights reserved.
doi:10.1016/j.jafrearsci.2009.07.010

to be related to both the impermeable, clay-rich host lithologies and their relatively shallow burial depth (Pearson et al., 2004, 2006). This discovery of excellently preserved and markedly diverse microfossil assemblages, in otherwise typical shelfal mudstone facies, represents a significant advance in our knowledge of the biodiversity and biostratigraphy of Upper Cretaceous–Neogene microfossils. Also, the TDP material provides a unique opportunity to reconstruct the subtropical temperature record through the Late Cretaceous–Neogene.

Previous TDP drilling seasons (2002–2005) targeted and recovered Paleocene-lower Oligocene sediments from around Kilwa and Lindi (Fig. 1a), as well as incomplete Upper Cretaceous (Albian–Cenomanian, Turonian, upper Campanian–lower Maastrichtian) sequences at TDP Sites 5 at Lindi and 9 and 15 at Kilwa (Pearson et al., 2004, 2006; Nicholas et al., 2006; Lees, 2007). These results were synthesized in Nicholas et al. (2006), who formally named and defined formations (Fm) in the clay-dominated, Upper Cretaceous–Paleogene Kilwa Group (Fig. 1b), and provided a preliminary sequence stratigraphy. New drilling around Lindi in 2007 demonstrated the presence of more stratigraphically-extensive Upper Cretaceous sediments than appreciated in previous years. We present here a synthesis of results from the 2007 season including the litho- and biostratigraphy of planktonic foraminifera and calcareous nannofossils, and chemostratigraphy for TDP Sites 21–26 and outcrop data. A total of 501.17 m of core was drilled in 2007, ranging from the upper Albian–upper Campanian, in addition to a thin Miocene–Pleistocene section. Also, isotopic evidence of partial recovery of Ocean Anoxic Event 2 (OAE2) (Schlanger and Jenkyns, 1976; Jenkyns, 1980), close to the Cenomanian–Turonian (C–T) transition, has been discovered in several of the new sites. Together, these results help constrain the poorly known Upper Cretaceous stratigraphy of southern Tanzania and establish a stratigraphic context for ongoing work that will examine Late Cretaceous extreme global warmth and proposed greenhouse glaciations.

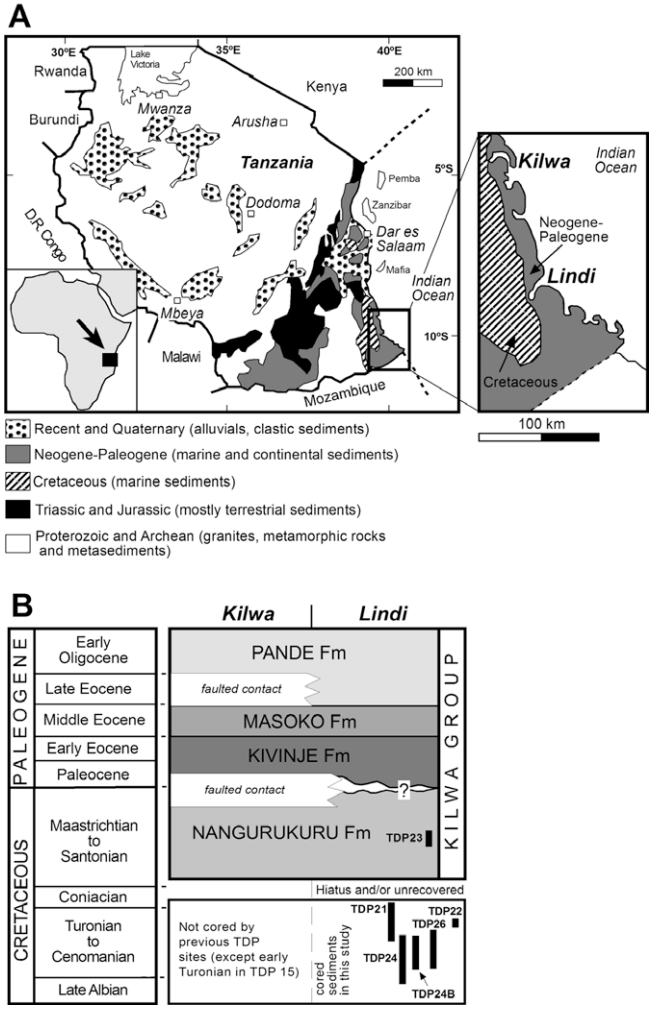

Fig. 1. Geographical and geological framework of the studied area: (a) synthesized geological map of Tanzania (modified from Schlüter, 2008) and close-up view of the Lindi–Kilwa region and (b) stratigraphic scheme from Nicholas et al. (2006) of the Cretaceous–Paleogene sediments in southern Tanzania, with the distribution of the sites drilled in 2007. TDP Site 25 corresponds to a Miocene–Pleistocene section and is not positioned in Fig. 1b.

2. Upper Cretaceous overview

The geology and depositional history of Tanzania are strongly influenced by the break up of Gondwana, beginning with an initial rifting phase about 300 Ma (Salman and Abdula, 1995, and references therein). A second rifting phase with active seafloor spreading from about 157 Ma separated Gondwana into western (South America and Africa) and eastern (Antarctica, India, Madagascar and Australia) blocks (Salman and Abdula, 1995), and the rifting of Madagascar away from East Africa led to development of a passive margin along what is now the Tanzanian coastal region. A marine transgression accompanied seafloor spreading in the second phase of rifting and resulted in deposition of thick Upper Jurassic and Lower Cretaceous sediments in a series of marginal basins that included the Mandawa and Rovuma basins in coastal areas of Tanzania and northern Mozambique (Salman and Abdula, 1995; Key et al., 2008). A major transgression during the Late Cretaceous caused widespread deposition of mudstones in offshore environments of the Mandawa and Rovuma basins that persisted into the Paleogene. A modern review of the tectonic history of coastal Tanzania can be obtained from Nicholas et al. (2007), with reference to deposition during the Late Cretaceous–Neogene. Also, Key et al. (2008) recently revised the lithostratigraphy of the Mesozoic and Cenozoic successions of the Rovuma basin in northern coastal Mozambique.

Cretaceous and Paleogene marine sediments crop out along most of the Tanzanian coastal region south of Dar es Salaam (Kent et al., 1971), and the most extensive exposures are along a continuous band between Kilwa and Lindi (Fig. 1a). Upper Cretaceous sediments in the area have been known since the first decades of the 1900s, but more detailed descriptions were not published until Moore et al. (1963), Gierlowski-Kordesch and Ernst (1987), Ernst and Schlüter (1989), and Ernst and Zander (1993). Schlüter (1997) named the Kilwa Group for the Upper Cretaceous sediments exposed around Kilwa, but neither divided them into formations nor defined their stratigraphic limits. Nicholas et al. (2006) ascribed the Upper Cretaceous rocks between Kilwa and Lindi to the Nangurukuru Fm (Santonian–Maastrichtian), while the Paleogene sediments were divided between the overlying Kivinje Fm, Masoko Fm and Pande Fm (Fig. 1b). In northern coastal Mozambique, Key et al. (2008) formally described the Upper Cretaceous sediments as belonging to the Mifume Fm (Albian–Maastrichtian).

Most significant to this work is the Nangurukuru Fm, which is typically composed of dark greenish gray, silty claystones interbedded with thin, hard, carbonate-cemented, fine- to coarse-grained sandstones that weather out to orange–brown tones (Nicholas et al., 2006). Bioturbation is common in the claystones, and the sandstones show a *Nereites* ichnofacies that has been suggested as indicating varying relative water depths (Gierlowski-Kordesch and Ernst, 1987; Ernst and Zander, 1993). Flutes, grooves and prod marks at the base and ripples on the top surfaces have been

described from the *Nereites* sandstones (Pearson et al., 2004, 2006; Nicholas et al., 2006) and interpreted as being deposited by turbulent flows in open marine settings.

One of the issues that still remains unresolved is definition of the base of the Nangurukuru Fm. Nicholas et al. (2006) suggested that its basal surface should lie at the lowest level of the Santonian claystones, marking the onset of an overall subsidence in the basin and sedimentation of the Kilwa Group. Currently, the oldest outcrop of the Santonian is found on the banks of the Matandu River near Kilwa (Nicholas et al., 2006). Exploration wells in southern coastal Tanzania, though, reported Aptian–Albian marls (Kingongo Marls) unconformably overlying Jurassic sediments onshore (Balduzzi et al., 1992) and Neocomian reservoir sands offshore (Mpanda, 1997). Also, previous TDP drilling in Kilwa recovered an ~100 m-thick pile of lower Turonian claystones (TDP15) and a single Cenomanian outcrop, but no Turonian or Coniacian surface exposures. Together, these observations led Nicholas et al. (2006) to propose that the Turonian package and the Aptian–Albian Kingongo Marls are separate units below a sequence boundary at the base of the Nangurukuru Fm, and that one or more disconformities might exist within the post-Albian–pre-Santonian sediments. In Lindi, a faulted disconformity was suggested for the contact between the Aptian–Albian Kingongo Marls and the overlying Campanian sediments of the Nangurukuru Fm (Nicholas et al., 2006).

From the sediments drilled in 2007, only the Campanian recovered at TDP Site 23 is included in the Nangurukuru Fm scheme of Nicholas et al. (2006) (Fig. 1b). Except for the thin Miocene–Pleistocene section of TDP Site 25, the rest of the new sites (TDP Site 21, 22, 24, 24B and 26) are ascribed to a separate stratigraphic unit underlying the Nangurukuru Fm (Fig. 1b), indicating that, at least in the Lindi region, the Cenomanian and Turonian sediments are more common, complete and expanded than suspected in previous works.

2.1. Revisions to the geological map of the Lindi region

Based on scarce sediment exposures and TDP cores, Nicholas et al. (2006, 2007) indicated that Upper Cretaceous and younger rocks strike NNW–SSE across Lindi bay, with younger sediments outcropping to the NE. The area is dominated by Kitulo Hill, a strike ridge that follows Maastrichtian–Paleocene sediments along its crest. To the E and NE of Kitulo Hill, the surface geology shows Paleocene–Eocene sediments of the Kivinje Fm, Masoko Fm and Pande Fm, in addition to unconformably overlying clays and limestones of Miocene and younger age (Nicholas et al., 2006, 2007). These authors also inferred two main oblique-slip faults that run NE–SW, almost perpendicular to the extension of Kitulo Hill. Another major NW–SE-trending fault was inferred to the SW of Kitulo Hill as marking a faulted contact between the base of the Nangurukuru Fm (upper Campanian) and the Aptian–Albian Kingongo Marls in Lindi.

The results of the 2007 expedition to Lindi confirm the major features of the geological map presented by Nicholas et al. (2007), but also suggest the need for a number of modifications (Figs. 2 and 3). To the W and SW of Kitulo Hill, the Upper Cretaceous sediments are not well exposed, with large parts of the explored area capped by a package of pale brown, medium- to fine-grained, loose sands with variable thicknesses (up to ~20 m). The absence of fossils in these sands allows no age control but, because they are easily recognized at the surface and unconformably overlie different parts of the Upper Cretaceous sequence, they may be much younger. To highlight the Upper Cretaceous sediments, this sand package has been omitted from the geological map shown here (Figs. 2 and 3). Accordingly, our data suggest an extensive Cenomanian–Maastrichtian sequence to the W and SW of Kitulo Hill that strikes NNW. A previous surface area assigned entirely to the planktonic foraminiferal *Gansserina gansseri* Zone (late Campanian–early Maastrichtian) (Nicholas et al., 2007) on the SW slope of Kitulo Hill has been subdivided here, its lower part now being attributed to the *Globotruncanella havanensis–Globotruncana aegyptiaca* Zones (late Campanian) (Figs. 2 and 3). To the SW of this area, several outcrop samples allow assignment of one sector to the *Globotruncana ventricosa* through *Radotruncana calcarata* Zones (early to late Campanian). Also, a small area on the SW side of Kitulo Hill is now ascribed to the *Abathomphalus mayaroensis* Zone (late Maastrichtian) (Figs. 2 and 3).

A wide surface sector, formally mapped as the Aptian–Albian Kingongo Marls (Nicholas et al., 2006; 2007), is largely assigned in this work to the *Helvetoglobotruncana helvetica–Marginotruncana schneegansi* Zones (early to late Turonian) (Figs. 2 and 3). On the NE side of this sector, though, the surface cores of TDP Sites 24, 24B and 26 yield older sediments belonging to the *Whiteinella archaeocretacea* Zone (earliest Turonian) (calcareous nannofossil zones UC6–8), and one surface sample 0.32 km to the N of TDP Site 24 yields the early Cenomanian foraminiferal marker *Rotalipora globotruncanoides*. This situation suggests that the northern part of this sector is affected by one or more faults that brought Cenomanian and lowermost Turonian sediments to the surface. The northern limit of this sector is also interpreted as a faulted contact with the area assigned to the *G. ventricosa–R. calcarata* Zones (early to late Campanian) (Figs. 2 and 3). That is, there is little space for Coniacian–Santonian sediments (theoretically located in between these two areas), although two isolated surface samples close to TDP Site 21 yielded the Santonian marker *Dicarinella asymetrica*, and the top core of this site contained foraminifera and nannofossils of Coniacian age. This situation points out that the extent of Coniacian–Santonian sediments in the Lindi area might be largely absent due to non-deposition or structural complications, or a thicker sequence may be present but not yet located.

Nicholas et al. (2007) reported significant regional structural complications in southern coastal Tanzania and proposed the existence of compressional tectonism since the Pliocene, possibly partly reactivating Triassic–Jurassic and Miocene faults. The local faulting inferred in the area of TDP Sites 24, 24B and 26 (Figs. 2 and 3), in addition to an Eocene faulted segment within the Turonian sequence of TDP Site 21 (see Section 4.1) (Fig. 4), may be associated with reactivation of older fault systems in Lindi (e.g., large fault south of Mitengi Bridge) (Nicholas et al., 2007) (Figs. 2 and 3). Further field seasons will examine the extension of local faulting in the Upper Cretaceous of Lindi, which is of general importance not only for regional tectonics, but also to foresee potential stratigraphic disruption when new drill sites are selected.

3. Methods

The new TDP sites were selected close to outcrops or surface samples that yielded well preserved foraminifera, with site numbers continuing from previous TDP drilling seasons. Continuous coring, using a rig with a practical penetration depth of 130 m, provided cores of up to 3 m long and 5 cm wide. The cores were photographed, described and sampled on site, and numbered from the surface down and divided into sections of up to 1 m, counting from the top. Samples for lithological, foraminiferal, nannofossil and geochemical analyses were collected with typical sample identifiers referring to the site, core number and section number. The position of a sample in any core and section is given as cm from the top of that section. Thus, TDP21/2/1, 5–10 cm indicates the interval at TDP Site 21 in core 2, Section 1 between 5 cm and 10 cm from the top of that section. Selected samples for foraminiferal and nannofossil analyses were processed for reconnaissance work at the well-site.

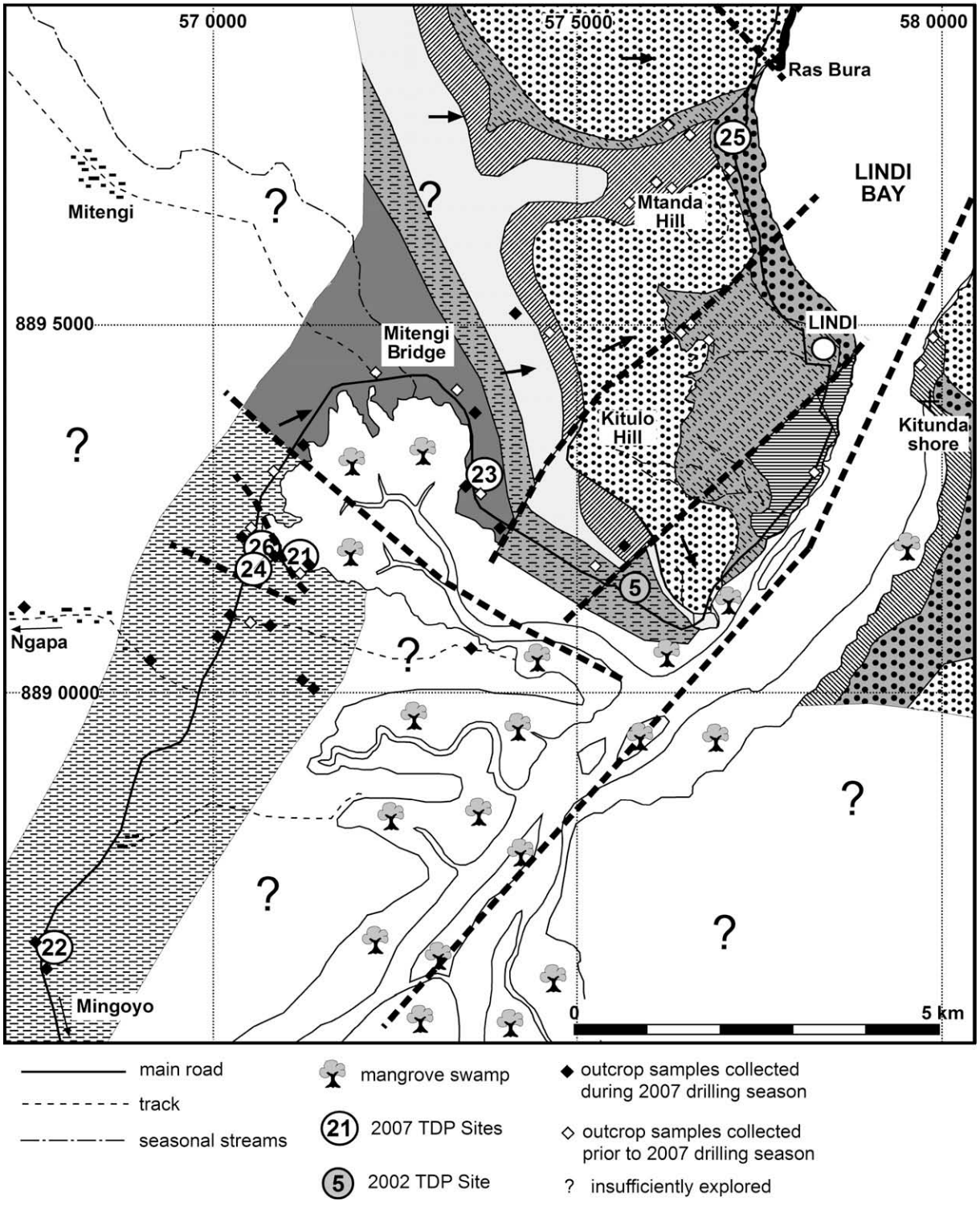

Fig. 2. Simplified geological map of the Lindi region, showing the distribution of the sites drilled in 2007. The map has been revised from Nicholas et al. (2007) (see main text). See Fig. 3 for map legend. Position of TDP Site 24B is masked by TDP Site 24.

The planktonic foraminiferal biozonation employed here follows that of Robaszynski and Caron (1995), with the addition of the *Pseudoguembelina palpebra* Zone of Huber et al. (2008), and the adoption of recent revisions in genus assignments, particularly those of Benitah-Lipson (2008). Table 1 summarizes age assignments of the foraminiferal events identified in this work according to the Ogg et al. (2004) time scale. Smear-slides were made as described in Bown and Young (1998) to study calcareous nannofossil assemblages. The nannofossil biozonation used here is the global scheme of Burnett et al. (1998) ('UC' zones), which has been calibrated with the proposed and ratified stage-boundary stratotype sections. A summary of the calcareous nannofossil events identified in this work is shown in Table 2. Minor disagreements occur between the foraminiferal and calcareous nannofossil age assignments, and these discrepancies will be addressed in more detailed, higher-resolution biostratigraphic analyses currently underway.

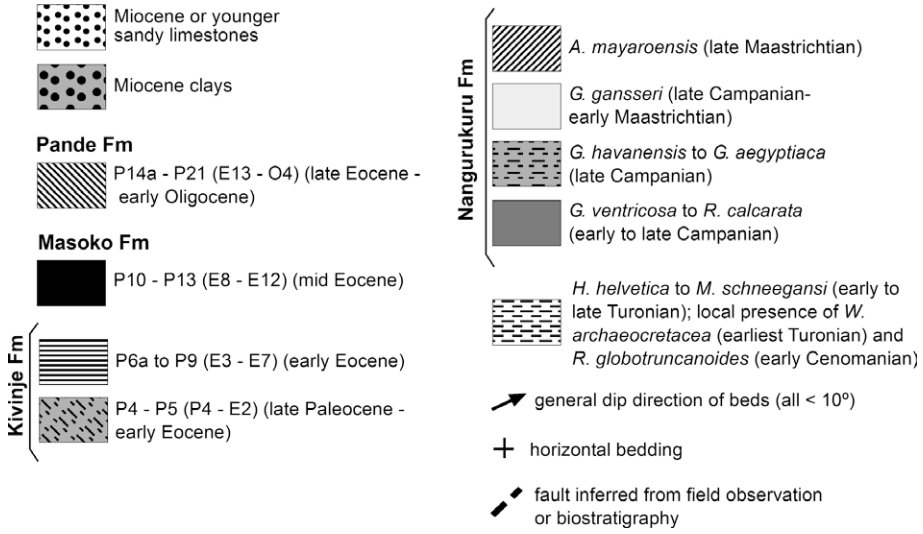

Fig. 3. Legend for geological map (Fig. 2).

Bulk samples were selected (~1 sample/core) to measure carbon and oxygen stable isotopes. For the organic carbon isotopes, decarbonated powdered samples (n = 189) were loaded into tin capsules and analyzed for $\delta^{13}C$ using a Carlo Erba 1500 Elemental Analyzer connected through a Finnegan Mat ConFlo II to a Delta Plus XL isotope ratio mass spectrometer, operated in continuous flow mode. Analytical precision (1 standard deviation), monitored through the determinations using acetanilide standards, was better than 0.1‰. For the carbonate carbon and oxygen isotopes, powdered samples (n = 143) were reacted in 103% H_2PO_4 at 70 °C in a Kiel III carbonate device, and the $\delta^{13}C$ and $\delta^{18}O$ of the evolved CO_2 were determined online in a Thermo Finnegan Delta Plus mass spectrometer. Analytical precision (1 standard deviation), based on uncorrected values of NBS-19 standards, was better than 0.07‰ for both $\delta^{13}C$ and $\delta^{18}O$. All the isotopic results are expressed in the standard δ-notation relative to the Vienna PDB standard.

4. Results

4.1. TDP Site 21

TDP Site 21 was drilled 0.6 km SE off the main road to Lindi and 7.6 km to the SW of Lindi (UTM 37L 571105, 8891863) (Fig. 2). The site is 0.1 km to the NE of a surface sample with the Santonian foraminiferal marker *D. asymetrica* and 0.68 km to the SE of a surface sample with the early Cenomanian marker *R. globotruncanoides*. Goals for this site were to drill the lower portion (Santonian) of the Nangurukuru Fm of Nicholas et al. (2006) and the contact with the Aptian–Albian Kingongo Marls. The site was drilled to 68.10 m, with good recovery between 8.10 m and 47.10 m, and moderate to poor recovery from the surface to 8.10 m and from 47.10 m to the bottom (Table 3). Drilling was stopped due to poor recovery in apparently unconsolidated sands with positive fluid pressures. Flow of fresh, effervescing water continued in this borehole at least until one year later.

4.1.1. Lithostratigraphy

The dominant lithologies from the surface to 39.97 m are medium to dark bluish gray, massive, silty claystones (Figs. 4, 5g, h), with faintly laminated intervals from 23.10 m to 35.10 m (see Section 5 and Table 10). A faulted segment is inferred from 20.10 m to 21.28 m (top of core TDP21/9) based on the presence of brown, massive claystones, whose color is ascribed to flow of oxidizing fluids. The interval from 39.97 m to the bottom of the hole contains light gray, massive- to normally-graded, fine- to medium-grained sandstones. Coarse-grained sandstones with normal gradation and matrix-supported, conglomeratic bases, with subangular to rounded pebbles, are also found from 44.10 m to 53.31 m (Figs. 4, 5a). Changes in the dip angle of the bedding planes and soft-sediment deformation are evident at several horizons from 41.10 m to 55.62 m. Small burrows and shell bioclasts are sporadically present.

4.1.2. Planktonic foraminiferal biostratigraphy

Despite the occurrence of *D. asymetrica* in a nearby surface sample, this Santonian–earliest Campanian species was not found in the subsurface at TDP Site 21. The latest Turonian–Coniacian *Dicarinella concavata* Zone is identified in core TDP21/1 (Fig. 4), based on the presence of the nominate taxon together with a number of marginotruncanid species (e.g., *Marginotruncana coronata, M. schneegansi*, M. *sinuosa*, and *Marginotruncana pseudolinneiana*). Except in one sample of core TDP21/3 (see below), cores 2 to the middle part of eight are assigned to the late Turonian *M. schneegansi* Zone (Fig. 4, Table 1), based on the: (1) dominance of foraminiferal assemblages by species of *Marginotruncana*, (2) presence of *Hedbergella simplex*, (3) absence of early-middle Turonian markers (e.g., *H. helvetica*, *Dicarinella hagni*, *W. archaeocretacea, W. aumulensis*, *Praeglobotruncana gibba*), and (4) absence of the latest Turonian–Coniacian marker *D. concavata*. Foraminiferal preservation in this zone ranges from moderate to good, with most shells showing calcite infilling and no intervals with glassy shell preservation.

An assemblage identical to that found in the *H. helvetica* Zone (see below) occurs in sample TDP21/3/1, 53–63 cm, between samples assigned to the *M. schneegansi* Zone (Fig. 4). It is unclear how this older interval came to be sandwiched between younger sediments, as there is neither slumping nor faulting evidence in this portion of the cores. Also, a lithological change (pale brown, semi-lithified, medium-grained sandstones overlying bluish gray silty claystones) is observed 13 cm above the sample with *H. helvetica* Zone (Fig. 4), but no features other than a normal lithological contact are visible.

Samples from the middle part of core TDP21/8 through 14 yield foraminiferal assemblages assigned to the early-middle Turonian *H. helvetica* Zone (Fig. 4; Table 1), based on the common occurrence of the nominate taxon with *D. hagni, Dicarinella imbricata, P. gibba, Whiteinella aprica, Whiteinella brittonensis* and *Whiteinella*

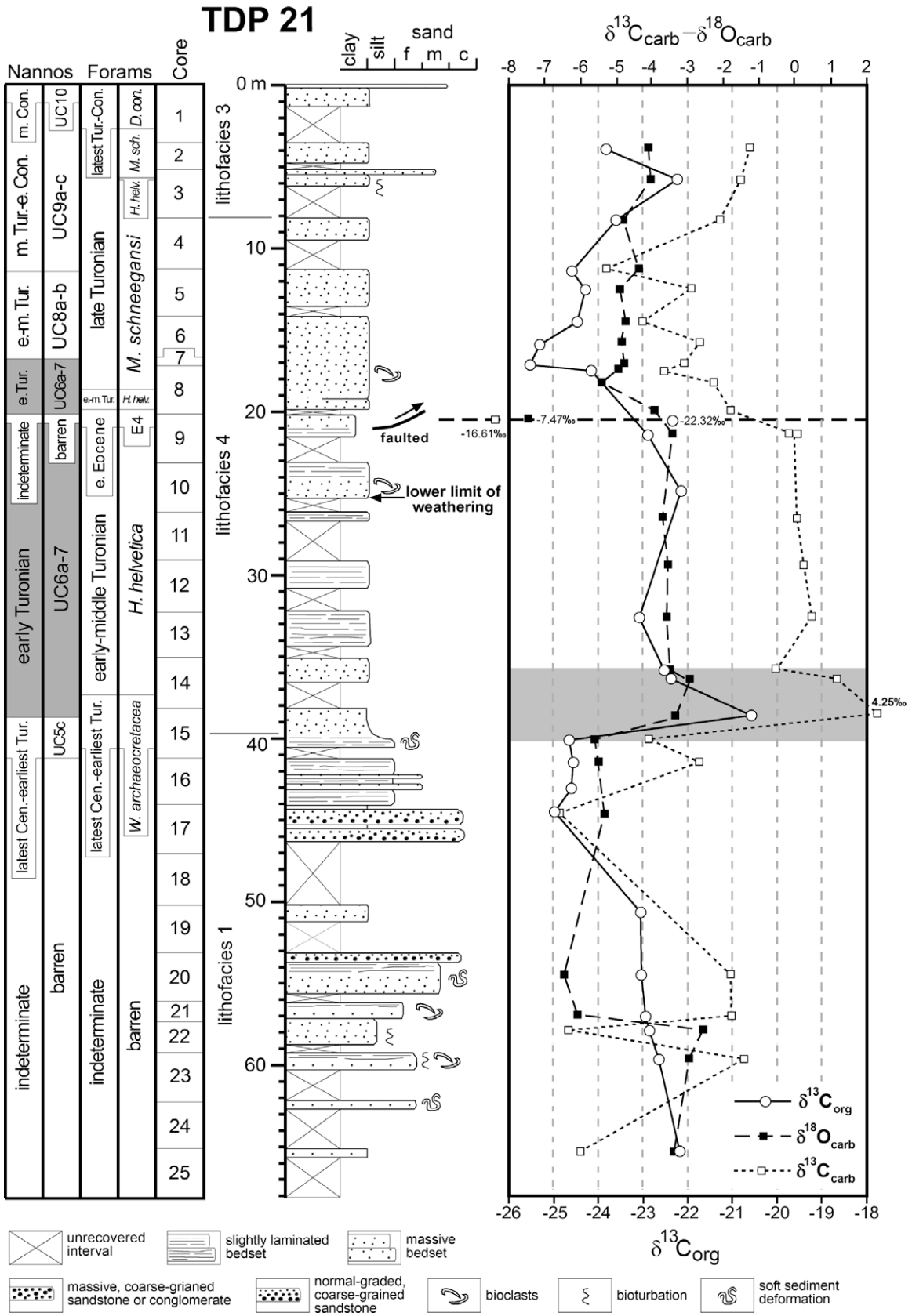

Fig. 4. Integrated lithostratigraphy, planktonic foraminiferal and calcareous nannofossil biostratigraphy, and chemostratigraphy of TDP Site 21. The lower limit of weathering indicated in core 10 marks the depth below which the cored sediments do not show weathering features (e.g., reddish coloration along fractures related to oxidizing fluids) due to modern Tanzanian weathering conditions. The interval highlighted in the columns showing calcareous nannofossil ages and zones contains assemblages correlatable among TDP Sites 21, 22, 24, 24B and 26. The gray shadow on the isotopic curves denotes the interval assigned to part of OAE2 isotopic excursions. Isotopic values of the sample from the Eocene slice are shown; m. Con.: middle Coniacian; e.-m. Con.: early-middle Coniacian; m. Tur.–e. Con.: middle Turonian–early Coniacian; e.-m. Tur.: early-middle Turonian; e. Tur.: early Turonian; *D. con.*: *D. concavata*; *H. helv.*: *H. helvetica*; *M. sch.*: *M. schneegansi*.

Table 1
Minimum, maximum and mean depths of core samples with or without planktonic foraminiferal First Appearance Datums (FADs) and Last Appearance Datums (LADs), together with estimated ages according to Ogg et al. (2004). Lowest and Highest Occurrences (LOs and HOs) represent observations of age diagnostic species, whose stratigraphic ranges are truncated in the TDP drillholes due to unconformities or barren intervals. The range truncation indicates that age estimates for the LOs and HOs are greater or less than the FAD and LAD ages.

Site	Planktonic foraminiferal event	Age (Ma)	Core sample (cm)	Minimum depth (m)	Maximum depth (m)	Mean depth
TDP23	*Radotruncana calcarata* HO	>74.47	23/1/1, 16–30	0.00	1.30	0.65
	Radotruncana calcarata FAD	75.57	23/7/1, 27–44	12.54	13.90	13.22
	Globotruncana ventricosa LO	<77.16	23/41/1, 13–43	88.53	88.53	88.53
TDP21	*Dicarinella concavata* FAD	90.79	21/1/1/70–80	0.80	4.82	2.81
	Marginotruncana coronata LO	<91.30	21/8/1, 66–76	17.86	19.33	18.60
	Helvetoglobotruncana helvetica HO	>91.51	21/8/3, 9–23	17.86	19.33	18.60
	Morozovella formosa LO	<54.00	21/9/1, 41–51	20.61	21.28	20.95
	Helvetoglobotruncana helvetica FAD	93.41	21/14/1, 76–93	36.03	38.78	37.41
	Whiteinella archaeocretacea LAD	93.95	21/15/1, 52–68	36.03	38.78	37.41
	Whiteinella archaeocretacea LO	<94.55	21/15/2, 41–57	39.67	41.59	40.63
TDP22	*Helvetoglobotruncana helvetica* HO	>91.51	22/5/1, 68–88	10.26	11.88	11.07
	Helvetoglobotruncana helvetica FAD	93.41	22/35/2, 52–69	91.39	92.88	92.14
	Whiteinella archaeocretacea LO	<94.55	22/51/2, 24–38	132.08	132.08	132.08
TDP26	*Whiteinella archaeocretacea* HO	>93.95	26/4/1, 30–52	2.11	5.42	3.77
	Whiteinella archaeocretacea LO	<94.55	26/5/1, 61–85	7.35	8.70	8.03
	Rotalipora cushmani HO	>93.95	26/6/1, 61–80	7.35	8.70	8.03
	Rotalipora cushmani LO	<95.33	26/21/3, 104–107	55.33	55.78	55.56
TDP24	*Whiteinella archaeocretacea* HO	>93.95	24/2/1, 20–34	1.37	2.34	1.86
	Whiteinella archaeocretacea LO	<94.55	24/4/1, 98–108	6.08	8.24	7.16
	Rotalipora cushmani HO	>93.95	24/5/1, 7–24	6.08	8.24	7.16
	Rotalipora cushmani LO	<95.33	24/24/2, 8–18	57.18	57.96	57.57
	Planomalina buxtorfi LO	>100.94	24/25/1, 25–36	57.18	57.96	57.57

Table 2
Top and bottom depths of core samples that mark calcareous nannofossil First Appearance Datums (FADs) and Last Appearance Datums (LADs), as well as the base of identified biozones.

Site	Calcareous nannofossil event	Core sample (cm)	Nannofossil zone	Top depth of sample (m)	Bottom depth of sample (m)
TDP23	*Uniplanarius trifidus* FAD	23/13/1, 8–23	Base UC15d^{TP}	21.18	21.33
	Uniplanarius sissinghii FAD	23/37/3, 40–42	Base UC15c^{TP}	78.50	78.52
TDP21	*Micula staurophora* FAD	21/1/1, 113–118	Base UC10	1.13	1.18
	Lithraphidites septenarius FAD	21/5/1, 18–20	Base UC9a	11.28	11.30
	Eiffellithus eximius FAD	21/7/1, 21–23	Base UC8a	16.81	16.83
	Helenea chiastia LAD	21/15/1, 68–71	Base UC6a	38.78	38.81
TDP26	*Eiffellithus eximius* FAD	26/2/1, 23–24	Base UC8a	2.13	2.14
	Helenea chiastia LAD	26/6/1, 91	Base UC6a	8.81	8.81
	Corollithion kennedyi LAD	26/7/1, 10–11	Base UC3e	11.00	11.01
	Staurolithites gausorhethium LAD	26/7/2, 16–17	Base UC3c	12.06	12.07
	Lithraphidites acutus FAD	26/21/1, 0–1	Base UC3a	53.00	53.01
TDP22	*Eprolithus moratus* FAD	22/45/2, 67–68	Base UC6b	118.37	118.38
TDP24	*Eprolithus moratus* FAD	24/4/2, 31–34	Base UC6b	6.31	6.34
	Helenea chiastia LAD	24/4/2, 38	Base UC6a	6.38	6.38
	Staurolithites gausorhethium LAD	24/5/1, 8	Base UC3c	8.08	8.08
	Lithraphidites acutus FAD	24/11/1, 22–23	Base UC3a	26.22	26.23
	Corollithion kennedyi FAD	24/19/1, 67–69	Base UC1a	49.37	49.39
	Arkhangelskiella antecessor FAD	24/27/1, 20–22	Base UC0b	62.20	62.22
TDP24B	*Eprolithus moratus* FAD	24B/2/1, 71–72	Base UC6b	2.71	2.72
	Corollithion kennedyi LAD	24B/3/1, 19–20	Base UC3e	5.19	5.20
	Staurolithites gausorhethium LAD	24B/4/1, 11–12	Base UC3c	8.11	8.12
	Lithraphidites acutus FAD	24B/11/1, 8–9	Base UC3a	29.08	29.09

praehelvetica, and absence of species of *Marginotruncana*. Most specimens in this interval are moderately preserved, with frequent infilling of calcite or pyrite. Nonetheless, several samples between cores TDP21/9 and 13 yield occasional specimens with no shell infilling and glassy preservation. Core TDP21/15 is assigned to the latest Cenomanian–earliest Turonian *W. archaeocretacea* Zone, based on the presence of the nominate taxon and absence of *H. helvetica*. Foraminifera are absent from samples between the top of core TDP21/16 and the bottom of the hole (Fig. 4).

The upper portion of core TDP21/9 is assigned to the early Eocene Zone E4 (*sensu* Berggren and Pearson, 2005) (Fig. 4, Table 1), due to the common presence of *Morozovella subbotinae*, *Morozovella formosa*, *Morozovella aequa*, *Subbotina patagonica*, and the absence of *Morozovella velascoensis* and *Morozovella aragonensis*. Preservation of this assemblage ranges from good to poor, with most specimens showing complete calcite infilling. The recognition that this interval is Eocene in age confirms that it represents a faulted slice.

4.1.3. Calcareous nannofossil biostratigraphy

The identification of nannofossil zone UC10 in core TDP21/1 indicates a youngest age of middle Coniacian (Fig. 4, Table 2). Cores TDP21/2–6 are assigned to UC9c–UC8a, which represent the early Coniacian–early Turonian. Below this interval, the undifferentiated

Table 3
Cored intervals in TDP Site 21.

Site	Core	Top (m)	Bottom (m)	Drilled (m)	Recovered (m)	Recovery (%)
TDP21/	1	0.00	3.50	3.50	1.37	39
	2	3.50	5.10	1.60	1.33	83
	3	5.10	8.10	3.00	1.09	36
	4	8.10	11.10	3.00	1.45	48
	5	11.10	14.10	3.00	2.50	83
	6	14.10	16.60	2.50	2.50	100
	7	11.60	17.10	5.50	5.50	100
	8	17.10	20.10	3.00	2.84	95
	9	20.10	23.10	3.00	1.57	52
	10	23.10	26.10	3.00	2.14	71
	11	26.10	29.10	3.00	0.62	21
	12	29.10	32.10	3.00	1.81	60
	13	32.10	35.10	3.00	2.36	79
	14	35.10	38.10	3.00	1.58	53
	15	38.10	41.10	3.00	2.37	79
	16	41.10	44.10	3.00	3.00	100
	17	44.10	47.10	3.00	2.25	75
	18	47.10	50.10	3.00	0.00	0
	19	50.10	53.10	3.00	1.00	33
	20	53.10	56.10	3.00	2.60	87
	21	56.10	57.20	1.10	1.10	100
	22	57.20	59.10	1.90	1.70	89
	23	59.10	62.10	3.00	1.35	45
	24	62.10	65.10	3.00	0.58	19
	25	65.10	68.10	3.00	0.58	19
	Total drilled: 68.10 m			Total recovered: 45.19 m		Recovery: 66%

(sub)zones UC6a–7 are recognized in cores TDP21/7–14 and assigned to the early Turonian (the base of UC7 is not identified here due to the apparent absence of *Quadrum gartneri*). Positive isotopic excursions that could be related to OAE2 (see below) occur in the lower part of UC6a–7. This interval is subject to further, intensive study, since preliminary data suggest a reduction in species richness that may be related to unusual surface-water conditions during OAE2, which cannot be explained by variable preservation.

One sample from the upper portion of core TDP21/9 is barren of nannofossils (Fig. 4), which corresponds to the foraminiferal sample of Eocene age discussed above; yet, nannofossils do not show any interruption to the stratigraphy either side of this barren level. Thus, the existence of this faulted Eocene slice does not seem to undermine the potential of TDP Site 21 for detailed biostratigraphic and paleoclimatic research. The oldest nannofossil subzone identified at this site is UC5c (latest Cenomanian–earliest Turonian) in core TDP21/15. The underlying cores TDP21/16–25 are barren of nannofossils, which is also the case for foraminifera. This situation is likely related to the existence of coarse-grained sediments through these cores, which are generally unsuitable for microfossil preservation. However, nannofossil preservation is generally good throughout the rest of the succession.

4.1.4. Chemostratigraphy

The bulk organic $\delta^{13}C$ ranges from −20.55‰ to −25.54‰ (average = −23.43‰ ± 1.20‰), and the curve shows low variability that is only interrupted by a significant change from the faulted Eocene segment to core TDP21/7, and across core TDP21/15 (Fig. 4). The latter excursion spans the latest Cenomanian–early Turonian and is likely related to part of the isotopic change due to OAE2. A positive trend is also seen from core TDP21/7 to the top of the profile. The bulk carbonate isotopic curves show higher variability. Data for $\delta^{13}C$ range from 4.25‰ to −6.56‰ (average = −2.07‰ ± 2.45‰), with an extremely low value in the Eocene slice (−16.61‰; excluded from statistics), and a remarkable positive change across core TDP21/15 possibly related to OAE2 (Fig. 4). Highly variable values occur from 40.40 m to the bottom of the hole (coarser sediments). Yet, higher isotopic values and much less variability are present along the rest of the curve, concurrent with finer lithologies. Data for $\delta^{18}O$ range from −2.59‰ to −6.47‰ (average = −4.31‰ ± 1.01‰) with lower values both in the Eocene slice (−7.47; excluded from statistics) and between 39.64 m and 56.95 m (coarser sediments) (Fig. 4). A positive change is also observed across core TDP21/15. The rest of the curve displays stable values coincident with finer lithologies. Given the correlation between finer lithologies and less variable bulk organic and carbonate isotopic data, the finer lithologies are considered the most likely to yield reliable foraminiferal isotopic data in this site.

4.2. TDP Site 22

TDP Site 22 was drilled 0.10 km E off the main road to Lindi, 13.30 km to the SE of Lindi (UTM 37L 567730, 8886659) (Figs. 2 and 3). The site is ~0.20 km to the NE of a surface sample with the early-middle Turonian marker *H. helvetica*. Goals for this site were to drill the lower portion of the Turonian and the upper part of the Cenomanian. After penetrating 11 m of fossil-barren, loose sands, this site was drilled to 134 m with good recovery in all cores (Table 4). Drilling was terminated in lithified, medium-grained sandstones due to slow coring near the penetration limit of the rig.

4.2.1. Lithostratigraphy

The dominant lithologies from 11 m to 109.80 m are mm- to cm-thick, interbedded, dark gray siltstones and fine-grained sandstones, with common, finely-laminated, organic-rich intervals (Figs. 5c, 6). The interval from 109.80 m to the bottom of the hole is composed of medium dark gray, moderately lithified, massive, medium-grained sandstones. Light gray, fine- to medium-grained sandstone partings with sharp, irregular basal surfaces are sporadically present. Moderate to intense soft-sediment deformation (e.g., bedding angle shifts, convoluted lamination, folded bedding) is abundant in the intervals 38.40–79.07 m and 95.70 m to the bottom of the hole (Fig. 6), and suggests relatively common processes of sediment liquidization before significant compaction took place. The intensity of stratigraphic disruption of these sediments is difficult to evaluate, since in 2007 no other holes were drilled close to

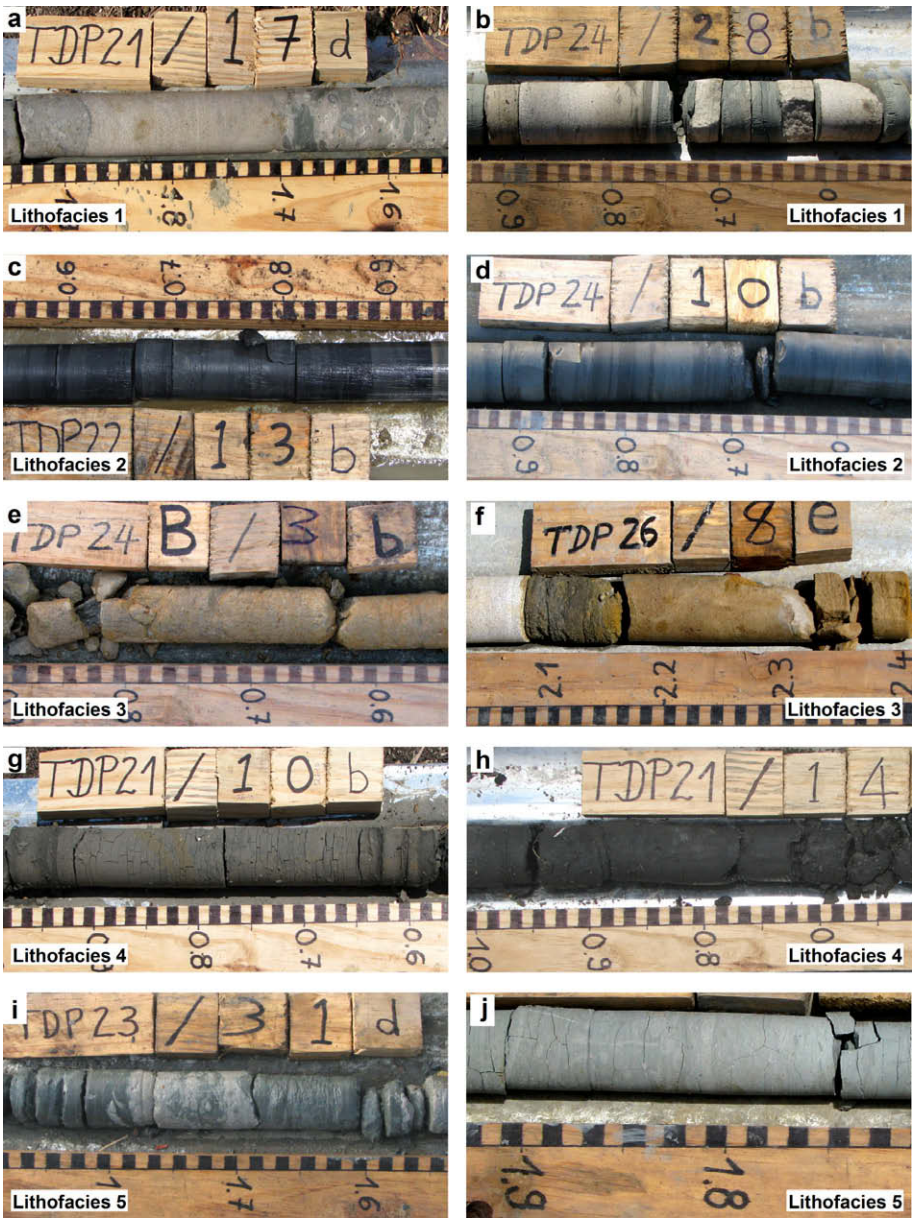

Fig. 5. Core photographs of representative intervals of the interpreted lithofacies 1–5 (see Section 5 and Table 10 for definition). In (a), note a sharp contact between two coarse sandstone layers at 1.88 m, and the conglomeratic character of the base of another layer between 1.55 m and 1.70 m. In (b), normal gradation and lamination at the top are visible in a layer between 0.75 m and 0.90 m. In (c) and (d), note existence of fine lamination at some levels. (e) and (f) Show massive sandstone layers with medium to coarse grain size. In (g) and (h), the massive character of bluish gray claystones is visible. (i) and (j) Show massive siltstones with, respectively, thin layers of gray, fine sandstones and bioturbation burrows. Ruler divisions are in cm.

TDP Site 22 that allowed examination of the lateral extension of the soft deformation. This issue, along with the driving causes of the sediment deformation, will be analyzed in future TDP expeditions. Ammonite and inoceramid debris are visible at 20.05 m and 26.90 m, respectively, and small bioclasts and bioturbation mottling occur sporadically.

4.2.2. Planktonic foraminiferal biostratigraphy

Foraminifera are absent in the interval with loose sands (cores TDP22/1–4), whereas they are common to rare in the samples analyzed below. Cores TDP22/5 through 35 (11–92.88 m) yield remarkably well preserved planktonic foraminifera that are diagnostic of the early-middle Turonian *H. helvetica* Zone (Fig. 6, Table 1). Most of the samples yield specimens with glassy shell preservation, in which shell infilling is rare. Samples from cores TDP22/36 through 51 (92.88–133.08 m) also consistently yield very well preserved foraminifera, with numerous specimens showing glassy preservation. This interval is assigned to the early Turonian *W. archaeocretacea* Zone (Fig. 6, Table 1) due to the presence of the nominate taxon along with *W. praehelvetica*, *D. hagni* and *D. imbricata*, and the absence of Cenomanian species of *Rotalipora, Thalamnninella* and *Parathalmanninella*.

4.2.3. Calcareous nannofossil biostratigraphy

Cores TDP22/1–4 are barren of nannofossils, but preservation in the underlying sediments is generally good. The rest of the section is assigned to the early Turonian (Fig. 6), based on the identification of undifferentiated UC6b(-7?) (cores TDP22/5–45) overlying UC6a (cores TDP22/45–51). The presence of the species *Eprolithus moratus* in core TDP22/45 is used to recognize the base of the

Table 4
Cored intervals in TDP Site 22.

Site	Core	Top (m)	Bottom (m)	Drilled (m)	Recovered (m)	Recovery (%)
TDP22/	1	0.00	2.00	2.00	1.50	75
	2	2.00	5.00	3.00	2.10	70
	3	5.00	8.00	3.00	1.10	37
	4	8.00	11.00	3.00	2.27	76
	5	11.00	14.00	3.00	3.00	100
	6	14.00	17.00	3.00	3.00	100
	7	17.00	19.60	2.60	2.30	88
	8	19.60	23.00	3.40	3.40	100
	9	23.00	26.00	3.00	3.00	100
	10	26.00	29.00	3.00	1.65	55
	11	29.00	32.50	3.50	1.90	54
	12	32.50	35.50	3.00	2.75	92
	13	35.50	38.50	3.00	2.55	85
	14	38.40	41.50	3.10	3.10	100
	15	41.50	44.50	3.00	2.84	95
	16	44.50	47.50	3.00	2.14	71
	17	47.50	50.50	3.00	2.81	94
	18	50.50	53.50	3.00	2.84	95
	19	53.50	54.30	0.80	0.80	100
	20	54.30	54.80	0.50	0.45	90
	21	54.80	56.70	1.90	1.86	98
	22	56.70	59.70	3.00	2.84	95
	23	59.70	60.70	1.00	1.00	100
	24	60.70	62.70	2.00	1.98	99
	25	62.70	65.70	3.00	2.96	99
	26	65.70	68.70	3.00	2.82	94
	27	68.70	71.70	3.00	2.43	81
	28	71.70	74.70	3.00	3.00	100
	29	74.70	77.70	3.00	2.80	93
	30	77.70	79.07	1.37	1.37	100
	31	79.07	80.70	1.63	1.57	96
	32	80.70	83.70	3.00	2.80	93
	33	83.70	86.70	3.00	2.63	88
	34	86.70	89.70	3.00	3.00	100
	35	89.70	92.70	3.00	2.39	80
	36	92.70	95.70	3.00	2.75	92
	37	95.70	98.70	3.00	3.00	100
	38	98.70	101.70	3.00	2.20	73
	39	101.70	103.00	1.30	1.14	88
	40	103.00	104.70	1.70	1.68	99
	41	104.70	107.70	3.00	2.64	88
	42	107.70	110.70	3.00	2.66	89
	43	110.70	113.70	3.00	2.91	97
	44	113.70	116.70	3.00	2.60	87
	45	116.70	119.70	3.00	2.85	95
	46	119.70	122.70	3.00	2.80	93
	47	122.70	125.70	3.00	2.35	78
	48	125.70	127.60	1.90	1.55	82
	49	127.60	128.70	1.10	1.10	100
	50	128.70	131.70	3.00	2.67	89
	51	131.70	134.00	2.30	1.40	61
	Total drilled: 134.00 m			Total recovered: 117.25 m		Recovery: 87.50%

UC6b subzone (Table 2). On the other hand, it is noteworthy that the interval assigned to UC6a–UC6b(-7?) in this site is hugely expanded (122 m thick) compared to the similar biozones in TDP Site 21 (21 m thick) (Fig. 4). This situation might be related to sediment reworking in TDP Site 22, associated with soft-sediment deformation (Fig. 6). An expanded interval in UC6 (early Turonian) was also seen in the previously-drilled TDP Site 15 (JAL, unpublished data), where it was associated with reworking of Albian–Cenomanian material.

4.2.4. Chemostratigraphy

The bulk organic $\delta^{13}C$ ranges from −21.66‰ to −23.23 (average = −22.59‰ ± 0.37‰) and the curve is characterized by a remarkable absence of variability (Fig. 6). Likewise, the bulk carbonate $\delta^{13}C$ and $\delta^{18}O$ curves show very low variability. Data for $\delta^{18}O$ range from −3.24‰ to −4.14‰ (average = −3.61‰ ± 0.22‰) and values for $\delta^{13}C$ range from 0.29‰ to −3.74‰ (average = −1.11‰ ± 1.26‰) with very stable values, except in two samples with low $\delta^{13}C$ at cores TDP22/12 (−3.37‰) and 30 (−3.74‰) (Fig. 6). The marked stability of the organic and carbonate isotopic curves, along with the relatively little lithological variability and excellent preservation of foraminifera in all samples, is an indication that this site may provide significant foraminiferal isotopic data for the Turonian, a widely debated interval where global warmth peaks and greenhouse glaciations have been proposed.

4.3. TDP Site 23

TDP Site 23 was drilled 0.10 km E off the main road to Lindi and 5.10 km to the W of Lindi (UTM 37L 573638, 8893108) (Figs. 2 and 3). The site was 0.31 km to the NE of a surface sample with the late Campanian marker *R. calcarata*. Goals for this site were to drill the upper and middle Campanian and try to reach Santonian sedi-

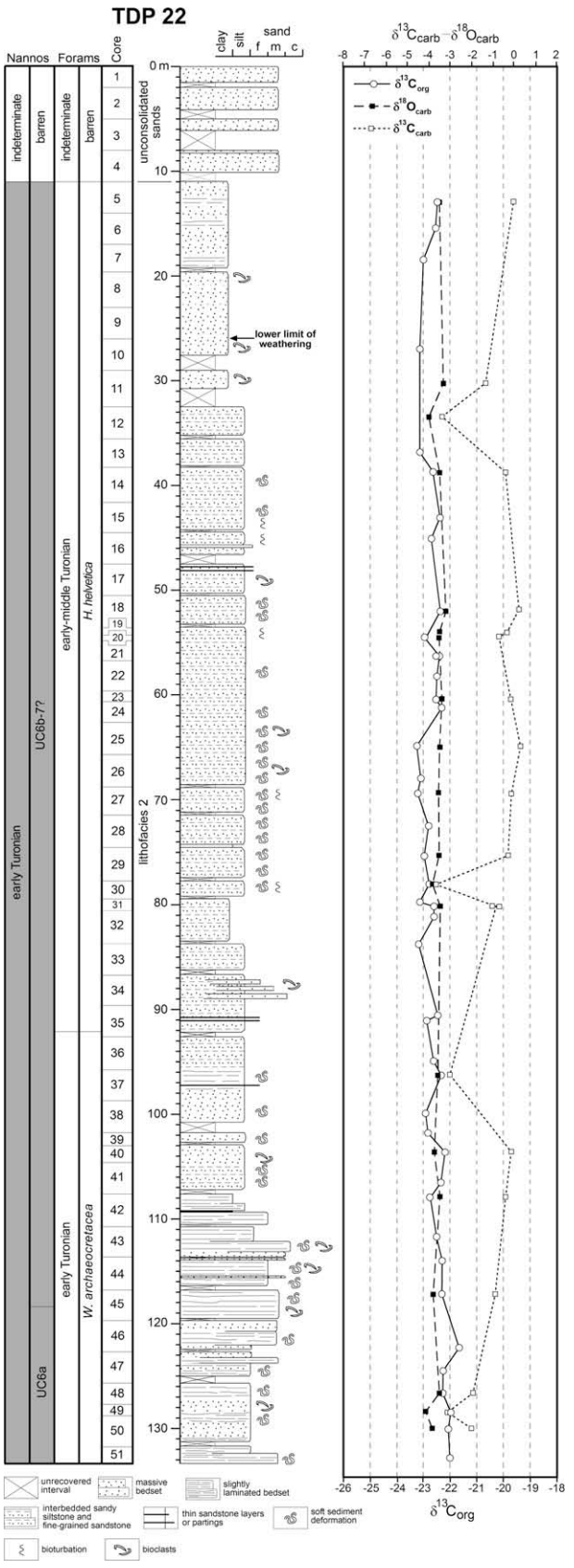

Fig. 6. Integrated lithostratigraphy, planktonic foraminiferal and calcareous nannofossil biostratigraphy, and chemostratigraphy of TDP Site 22. Lower limit of weathering in core 9 indicated.

ments at the base of the Nangurukuru Fm of Nicholas et al. (2006). The site was drilled to 90.70 m with good recovery along the entire hole except for two intervals with moderate to poor recovery between 4.10 m and 10.70 m, and 20.10 m and 21.10 m (Table 5). Drilling was stopped due to very slow coring in apparently lithified sandstones.

4.3.1. Lithostratigraphy

The principal lithologies from the surface to 64.10 m are pale blue to grayish blue-green, massive, calcareous claystones with relatively common small bioturbation mottling and bioclasts (Figs. 5i, 7). The interval from 57.10 m to 64.10 m presents significant cementation as well as frequent layers (1–10 cm thick) of light gray, medium- to fine-grained, massive sandstones with sharp, irregular contacts (Fig. 5i). On the other hand, the bottom of the hole (64.10–90.70 m) consists of greenish gray and light bluish gray, weakly-bedded, massive siltstones–sandy siltstones, where mm- to cm-sized, bioturbation burrows are relatively abundant (Figs. 5j, 7). These burrows are mostly elongate or oval and bedding-parallel, but simple sub-vertical burrows are also present. Small bioclasts are common in this interval.

4.3.2. Planktonic foraminiferal biostratigraphy

Foraminifera are abundant in all the clayey siltstone samples analyzed from this site. Assemblages assigned to the late Campanian *R. calcarata* Zone range from core TDP23/1–8 (the upper 13.90 m of the hole) (Fig. 7, Table 1). Specimens in this interval show moderate to good preservation, with mostly infilled shells and occasional glassy shells and no infilling. All underlying cores (TDP23/8 to the bottom of the hole) are assigned to *G. ventricosa* Zone (late early Campanian) (Fig. 7) due to the co-occurrence of the nominate species with *Globotruncanita elevata* and the absence of *R. calcarata*. The majority of the specimens observed in this zone are moderately preserved and mostly or completely infilled with calcite. Hollow, glassy specimens are rarely found in the more clay-rich samples of cores TDP23/8 through 14 and 24.

4.3.3. Calcareous nannofossil biostratigraphy

Nannofossils observed in the samples from this site show good preservation and allow stratigraphic division into three subzones, UC15d^{TP}–UC15b^{TP}, which correspond to a late to early Campanian age (Fig. 7, Table 2).

4.3.4. Chemostratigraphy

The bulk organic $\delta^{13}C$ ranges from −23.94‰ to −26.77‰ (average = −25.27‰ ± 0.68‰) and the curve displays low variability only interrupted by minor changes in cores TDP23/38, 28, 22 and 17 (Fig. 7). A subtle positive trend is seen from core TDP23/14–8. The bulk carbonate $\delta^{18}O$ ranges from −2.07‰ to −4.61‰ (average = −3.08‰ ± 0.60‰) and the profile shows low variability with minor negative changes at cores TDP23/33, 22 and 13 (Fig. 7). The bulk carbonate $\delta^{13}C$ ranges from 1.81‰ to −2.16‰ (average = −0.28‰ ± 1.02‰) and the curve exhibits low variability except from core TDP23/22 through 1.

4.4. TDP Site 24

TDP Site 24 was drilled 0.03 km E off the main road to Lindi, 0.63 km to the W of TDP Site 21 and 8.5 km to the SW of Lindi (UTM 35L 570474, 8891859) (Figs. 2 and 3). The goal was to drill the C–T boundary interval by locating the site down section from TDP Site 21, which had provided microfossil assemblages around this interval (Fig. 4). The site was drilled to 74 m, with good recovery between 20 m and 68 m, and moderate to poor recovery from the surface to 20 m and from 68 m to the bottom of the hole (Table 6). Drilling was stopped in hard, lithified coarse sandstones of Albian age.

Table 5
Cored intervals in TDP Site 23.

Site	Core	Top (m)	Bottom (m)	Drilled (m)	Recovered (m)	Recovery (%)
TDP23/	1	1.00	2.65	1.65	1.36	82
	2	2.65	4.10	1.45	1.45	100
	3	4.10	6.10	2.00	1.00	50
	4	6.10	9.10	3.00	1.60	53
	5	9.10	10.70	1.60	0.10	6
	6	10.70	12.10	1.40	1.40	100
	7	12.10	13.70	1.60	1.47	92
	8	13.70	15.10	1.40	1.30	93
	9	15.10	16.60	1.50	1.45	97
	10	16.60	18.10	1.50	1.50	100
	11	18.10	20.10	2.00	2.00	100
	12	20.10	21.10	1.00	0.05	5
	13	21.10	24.10	3.00	2.55	85
	14	24.10	27.10	3.00	2.99	100
	15	27.10	30.10	3.00	2.70	90
	16	30.10	30.30	0.20	0.20	100
	17	30.30	31.30	1.00	0.45	45
	18	31.30	33.30	2.00	1.79	90
	19	33.30	34.90	1.60	1.60	100
	20	34.90	36.30	1.40	1.40	100
	21	36.30	36.90	0.60	0.60	100
	22	36.90	39.90	3.00	3.00	100
	23	39.90	42.90	3.00	3.00	100
	24	42.90	45.90	3.00	3.00	100
	25	45.90	48.90	3.00	3.00	100
	26	48.90	51.90	3.00	2.70	90
	27	51.90	54.50	2.60	1.96	75
	28	54.50	55.10	0.60	0.45	75
	29	55.10	57.10	2.00	1.90	95
	30	57.10	58.10	1.00	0.87	87
	31	58.10	61.10	3.00	2.58	86
	32	61.10	64.10	3.00	2.72	91
	33	64.10	67.10	3.00	2.60	87
	34	67.10	70.10	3.00	2.12	71
	35	70.10	73.10	3.00	2.95	98
	36	73.10	76.10	3.00	2.90	97
	37	76.10	79.10	3.00	2.91	97
	38	79.10	82.10	3.00	3.00	100
	39	82.10	85.10	3.00	3.00	100
	40	85.10	88.10	3.00	2.16	72
	41	88.10	90.70	2.60	1.10	42
	Total drilled: 90.70 m			Total recovered: 76.88 m		Recovery: 84.76%

4.4.1. Lithostratigraphy

The dominant lithologies from the surface to 62 m (core TDP24/26) are mm- to cm-thick, interbedded, dark gray siltstones and fine-grained sandstones (Figs. 5d, 8). A few layers (cm-thick) of light brown, fine-grained sandstones occur in the top portion of the section (from the surface to 11 m). Bioturbation and bioclasts are rare through this interval. Well-lithified, sandy siltstones with common cross-cutting, sulfate–carbonate veins and fractures occur from 62 m to 65 m (core TDP24/27) (Fig. 8). From 65 m to the bottom of the hole, light gray, lithified, coarse-grained sandstones with woody debris and rip-up clasts are interbedded with greenish gray siltstones (Figs. 5b, 8). The sandstone beds have sharp, irregular basal contacts, while small bioturbation mottling is only visible in the siltstone layers.

4.4.2. Planktonic foraminiferal biostratigraphy

Planktonic foraminifera from cores TDP24/1 to the uppermost part of five (0–7.16 m) are diagnostic of the *W. archaeocretacea* Zone (early Turonian) (Fig. 8; Table 1) due to the co-occurrence of the nominate taxon with *H. praehelvetica* and the absence of *H. helvetica.* An unconformity is placed at 7.16 m below the surface (Fig. 8), where a foraminiferal assemblage indicative of the lower part of the *Rotalipora cushmani* Zone (middle-late Cenomanian) (e.g., presence of *Thalmanninella greenhornensis*, *Thalmanninella globotruncanoides* and *Rotalipora montsalvensis*, but absence of forms appearing in the upper portion of the zone, including *Thalmanninella deeckei*, *P. gibba*, *Dicarinella algeriana* and *Whiteinella* spp.) occurs immediately below samples assigned to the *W. archaeocretacea* Zone. Throughout the *R. cushmani* Zone of this site (lower part of core TDP24/4 to through 24) (7.16–57.57 m) (Fig. 8), foraminifera are abundant and generally show good preservation, with occasional occurrence of specimens with glassy shells and no infilling.

A second unconformity is placed at 57.57 m below the surface (Fig. 8), based on: (1) the absence of assemblages indicative of the *R. globotruncanoides* Zone (early Cenomanian) and *R. reicheli* (middle Cenomanian) Zones in any of the samples studied, and (2) the presence of late Albian foraminifera of the *Planomalina buxtorfi* Zone, including the nominate taxon and *R. ticinensis*, from 57.57 m to the bottom of the hole. In the upper Albian samples, foraminifera are rare and preservation is poor to moderate with all specimens showing shell recrystallization and calcite or pyrite infilling.

4.4.3. Calcareous nannofossil biostratigraphy

Nannofossils are well preserved in the samples studied from this site. The top of the hole (cores TDP24/1–4) is represented by the early Turonian subzones UC6b(-7?) and UC6a (Fig. 8, Table 2), which correlate with isotopic excursions related to OAE2 (see below), as observed in TDP Site 21 (Fig. 4). The unconfor-

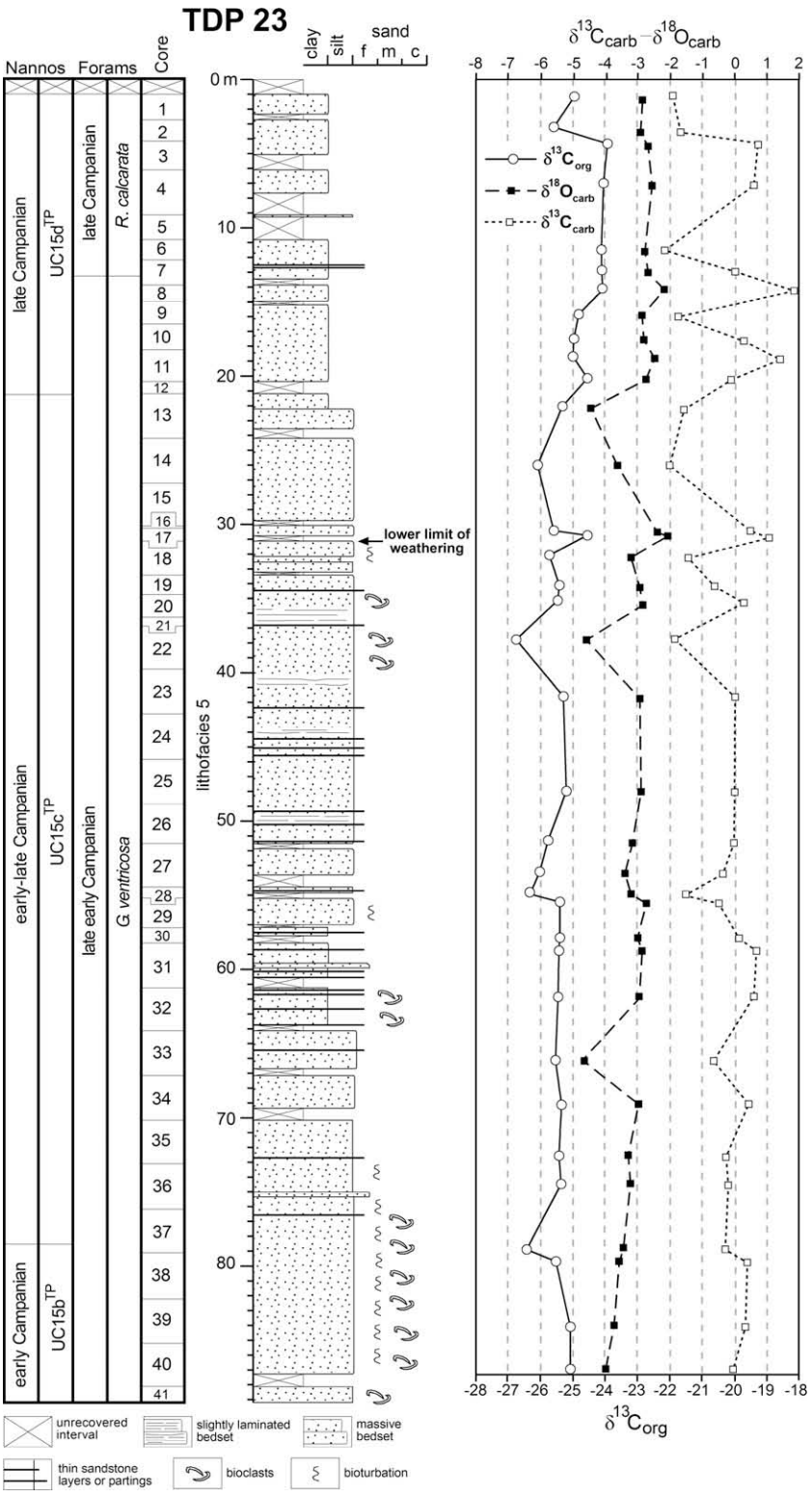

Fig. 7. Integrated lithostratigraphy, planktonic foraminiferal and calcareous nannofossil biostratigraphy, and chemostratigraphy of TDP Site 23. Lower limit of weathering in core 17 indicated.

mity previously postulated within core TDP24/4 is marked by the major condensation of UC3c–5c, representing the late Cenomanian–earliest Turonian. Below this interval, an early to late Cenomanian succession is indicated by UC1a–UC3b. The presence of UC0c, indicative of the latest Albian–early Cenomanian, seems to imply a complete boundary interval, in contrast to the interpretation of unconformity presented by the foraminifera. The late Albian (UC0a–UC0b) is also present in this hole (Fig. 8, Table 2). Finally, part of the cores TDP24/28 and 29 are barren of nannofossils.

Table 6
Cored intervals in TDP Site 24.

Site	Core	Top (m)	Bottom (m)	Drilled (m)	Recovered (m)	Recovery (%)
TDP24/	1	0.00	2.00	2.00	1.37	69
	2	2.00	3.00	1.00	0.53	53
	3	3.00	5.00	2.00	1.18	59
	4	5.00	8.00	3.00	1.50	50
	5	8.00	11.00	3.00	1.00	33
	6	11.00	14.00	3.00	1.69	56
	7	14.00	17.00	3.00	1.20	40
	8	17.00	20.00	3.00	1.92	64
	9	20.00	23.00	3.00	2.35	78
	10	23.00	26.00	3.00	2.46	82
	11	26.00	29.00	3.00	2.84	95
	12	29.00	32.00	3.00	2.37	79
	13	32.00	35.00	3.00	3.00	100
	14	35.00	38.00	3.00	3.00	100
	15	38.00	41.00	3.00	2.53	84
	16	41.00	44.00	3.00	3.00	100
	17	44.00	47.13	3.13	3.13	100
	18	47.13	48.70	1.57	1.57	100
	19	48.70	50.00	1.30	0.96	74
	20	50.00	51.80	1.80	1.64	91
	21	51.80	53.00	1.20	1.20	100
	22	53.00	54.60	1.60	1.60	100
	23	54.60	56.00	1.40	1.27	91
	24	56.00	57.60	1.60	1.60	100
	25	57.60	59.00	1.40	1.13	81
	26	59.00	62.00	3.00	2.40	80
	27	62.00	65.00	3.00	2.92	97
	28	65.00	68.00	3.00	2.14	71
	29	68.00	71.00	3.00	1.35	45
	30	71.00	74.00	3.00	0.23	8
	Total drilled: 74.00 m			Total recovered: 55.08 m		Recovery: 74.43%

4.4.4. Chemostratigraphy

The bulk organic $\delta^{13}C$ ranges from −20.73‰ to −24.93‰ (average = −23.08‰ ± 0.92‰), and the curve displays relatively low variations along the entire section, except from 12.62 m to the surface (Fig. 8). Here, a positive excursion with two peaks (2.06‰ total shift) is visible and ascribed to part of the isotopic change associated with OAE2. The bulk carbonate isotopic records show higher variability (Fig. 8). Values range from 0.92‰ to −7.16‰ (average = −2.37‰ ± 1.68‰) for $\delta^{13}C$ and from −3.43‰ to −6.96‰ (average = −4.44‰ ± 0.73‰) for $\delta^{18}O$. Like the bulk organic $\delta^{13}C$, the bulk carbonate isotopic data exhibit positive excursions from 12.62 m to the surface. Thus, the presence of isotopic excursions indicative of partial recovery of OAE2, together with the generally good microfossil preservation throughout this interval, suggests that TDP Site 24 may give valuable foraminiferal isotopic data for the Cenomanian and early Turonian, a critical interval associated with extreme global warmth and enhanced organic carbon burial.

4.5. TDP Site 24B

TDP Site 24B was drilled 7 m to the N and uphill of TDP Site 24 (Figs. 2 and 3). The goal for this site was to get good recovery in the top cores to try to improve the record across the C–T boundary interval previously partially drilled in the surface cores of TDP Site 24 (Fig. 8). Because of the proximity of these two sites, the foraminiferal zonation in TDP Site 24B was expected to be identical to TDP Site 24. Thus, only samples for stable isotopes and nannofossils were collected. The site was drilled to 35 m, with good recovery from 8 m to 11 m and from 17 m to the bottom of the hole, and moderate recovery from the surface to 8 m and from 11 m to 17 m (Table 7). Drilling was terminated in apparently lithified siltstones when coring became exceptionally slow.

4.5.1. Lithostratigraphy

Like TDP Site 24, the dominant lithologies in TDP Site 24B are mm- to cm-thick, interbedded, dark gray siltstones and fine-grained sandstones (Fig. 9). A light brown, fine- to medium-grained sandstone interval is visible between 5 m and 7.42 m (Figs. 5e, 9). A few light gray, fine-grained sandy partings also appear throughout the cores. No bioturbation or fossils are observed.

4.5.2. Calcareous nannofossil biostratigraphy

Preservation of nannofossils is generally good throughout this site. The top of the hole (core TDP24B/1 and uppermost part of 2) is assigned to the early Turonian subzone UC6b(-7?), which occurs with high organic $\delta^{13}C$ values, possibly due to OAE2 (Fig. 9, Table 2). Below this unit, a condensed portion assigned to the late Cenomanian–early Turonian (UC3c–UC6a) is present (cores TDP24B/2–3). Then, a relatively expanded interval of middle to late Cenomanian (UC3a–b Zones) (cores TDP24B/4 to uppermost part of 11) lies above a thin early Cenomanian (UC1a–2c) unit (cores TDP24B/11–12). All these features allow a good correlation between TDP Sites 24B and 24.

4.5.3. Chemostratigraphy

The bulk organic $\delta^{13}C$ ranges from −21.54‰ to −23.99‰ (average = −22.93‰ ± 0.58‰) and the curve shows low variability from the bottom of the section to 8.09 m (Fig. 9). From this point to 2.72 m, a positive excursion (2.05‰ total shift) is observed and attributed to part of the isotopic shift due to OAE2. Then, the isotopic curve returns to pre-excursion values for the uppermost sample. A bulk organic $\delta^{13}C$-based correlation between TDP Site 24B and 24 (Fig. 11) reveals at least four tie-points across the isotopic profiles and indicates that these sites may be useful to study the broadly debated issues of cause and effect of OAE2. On the other hand, the bulk carbonate $\delta^{13}C$ ranges from −0.80‰ to −2.91‰

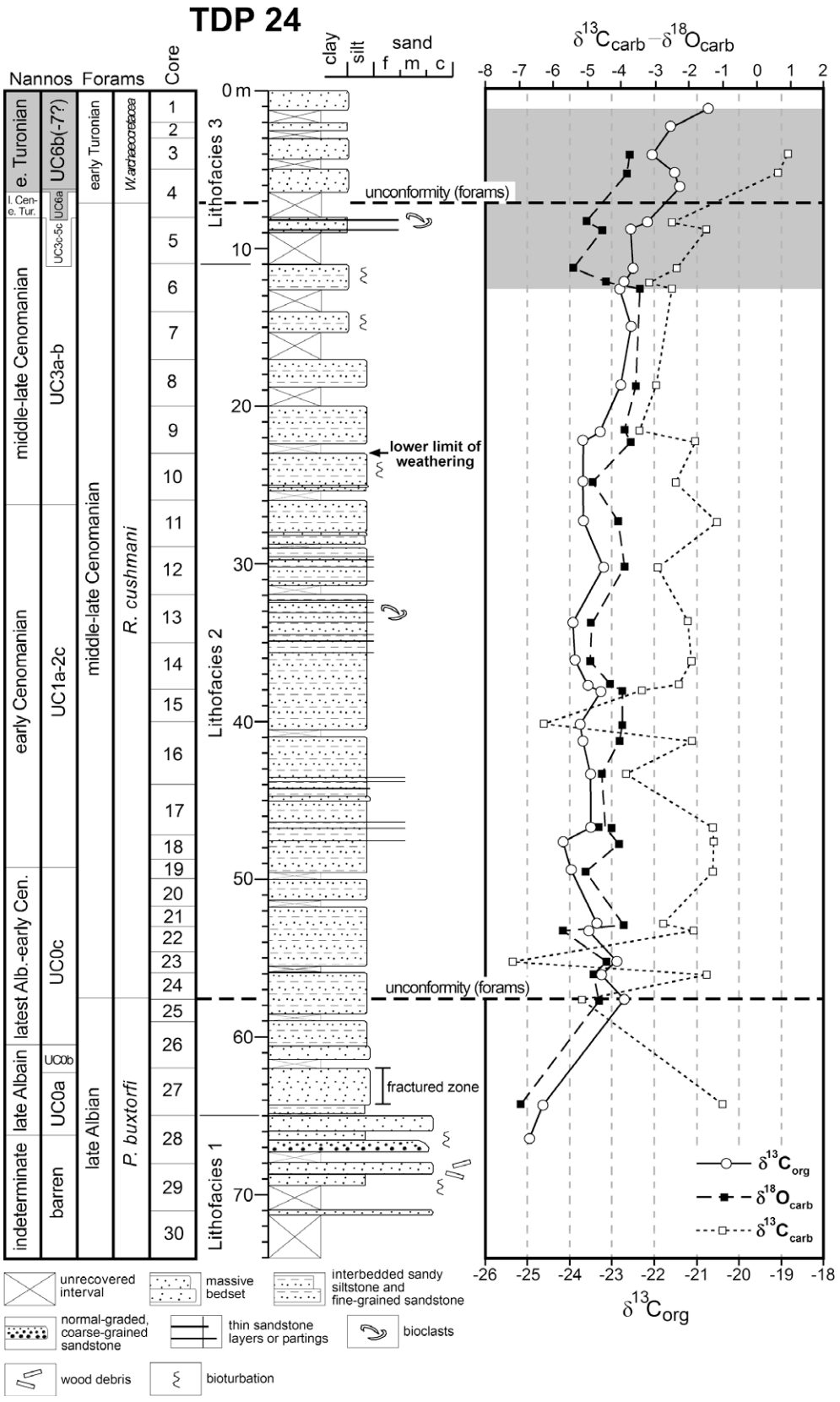

Fig. 8. Integrated lithostratigraphy, planktonic foraminiferal and calcareous nannofossil biostratigraphy, and chemostratigraphy of TDP Site 24. Lower limit of weathering in core 10 indicated. The gray shadow on the isotopic curves as in Fig. 4; e. Turonian: early Turonian; l. Cen.–e. Tur.: late Cenomanian–earliest Turonian; latest Alb.-early Cen.: latest Albian–early Cenomanian.

(average = −1.89‰ ± 0.85‰) and the $\delta^{18}O$ ranges from −3.52‰ to −5.87‰ (average = −4.96‰ ± 0.79‰). Both isotopic profiles display negative trends upwards, but no relationship is visible with the organic $\delta^{13}C$ profile (Fig. 9).

Table 7
Cored intervals in TDP Site 24B.

Site	Core	Top (m)	Bottom (m)	Drilled (m)	Recovered (m)	Recovery (%)
TDP24B/	1	0.00	2.00	2.00	1.15	58
	2	2.00	5.00	3.00	1.65	55
	3	5.00	8.00	3.00	2.42	81
	4	8.00	11.00	3.00	2.60	87
	5	11.00	14.00	3.00	1.71	57
	6	14.00	17.00	3.00	1.70	57
	7	17.00	20.00	3.00	2.42	81
	8	20.00	23.00	3.00	2.40	80
	9	23.00	26.00	3.00	3.00	100
	10	26.00	29.00	3.00	1.52	51
	11	29.00	32.00	3.00	2.45	82
	12	32.00	35.00	3.00	2.10	70
	Total drilled: 35.00 m			Total recovered: 25.12 m		Recovery: 71.77%

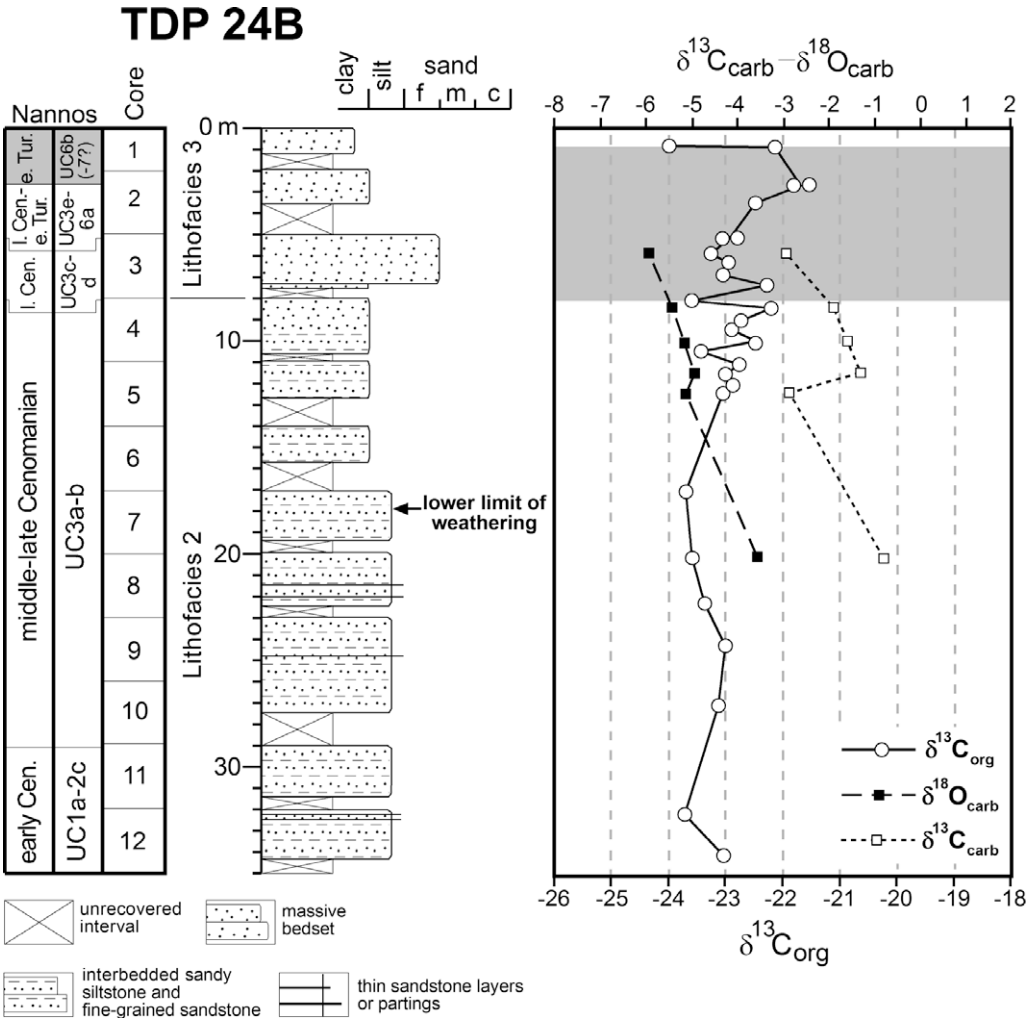

Fig. 9. Integrated lithostratigraphy, calcareous nannofossil biostratigraphy, and chemostratigraphy of TDP Site 24B. Lower limit of weathering in core 7 indicated. The gray shadow on the isotopic curves as in Fig. 4; e. Tur.: early Turonian; l. Cen.–e. Tur.: late Cenomanian–early Turonian.

4.6. TDP Site 25

TDP Site 25 was drilled in a small valley 0.11 km west off the main road to Lindi, 3.6 km north of Lindi (UTM 35L, 577282, 8898480) (Figs. 2 and 3). The site was selected to try to core across the Cretaceous–Tertiary (K–T) boundary, which was unsuccessfully attempted at TDP Site 5 on the south side of Kitulo Hill (Pearson et al., 2004). Previous TDP surveys reported the existence of Miocene clays disconformably underlain by upper Maastrichtian and lower Paleocene sediments in the area of TDP Site 25 (Nicholas et al., 2006). Positioning the rig on the Miocene clays would provide a possibility to record the K–T boundary interval some distance below the surface. However, at TDP Site 25, only Miocene or younger sediments were found and, due to drilling difficulties, drilling was terminated at 43.20 m (Table 8) without any Cretaceous cored. We summarize here the litho- and biostratigraphy, but will not discuss this site in subsequent sections due to the absence of Cretaceous sediments.

4.6.1. Lithostratigraphy

TDP Site 25 is characterized by extremely low recovery in the upper 23 m (cores TDP25/1–9) (Fig. 10), where only fragments of well-lithified, grayish orange, fossiliferous (e.g., coral and bivalve fragments) limestones mixed with drill mud were cored. Because the rig was positioned at the base of a valley and the recovery was so low, it is not known if these sediments are in place or form part of a large colluvial system of Recent age. No indication of misplaced sediments, though, is found from 23 m to 41.13 m (cores TDP25/9–17), which show medium gray, fossiliferous (e.g., individual corals, bryozoan and bivalve fragments), massive grainstones with common mm- to cm-sized mould and vug porosity, alternating with dark gray, slightly cemented, massive mudstones. From core TDP25/14 downwards, a remarkable reduction in porosity and increase in compaction is observed and both grainstone and mudstone intervals are much more lithified.

4.6.2. Planktonic foraminiferal biostratigraphy

Samples analyzed from cores TDP25/12 and 16 contain abundant planktonic and benthic foraminifera with glassy shells. They are assigned to late Miocene Zone M13 (Fig. 10), due to the presence of *Sphaeroidinellopsis disjuncta*, which ranges from Zone M5 to M13, together with *Globigerinoides sacculifer*, *Globigerinoides ruber*, *Globigerinella siphonifera*, *Globorotalia menardii* and *Orbulina universa*, which range from Zone M13a (late Miocene) to the Present.

4.6.3. Calcareous nannofossil biostratigraphy

A sample from core TDP25/2 yields a mixed assemblage of rare Cretaceous and Paleogene nannofossils, which probably represent reworking within sediments that contain no *in situ* components. Core TDP25/16 is Pleistocene in age (nannofossil zone NN19 of Martini, 1971) (Fig. 10), based on a well preserved, abundant nannofossil assemblage, containing *Pseudoemiliania lacunosa*, *Helicosphaera sellii* and small *Gephyrocapsa*, and lacking *Calcidiscus macintyrei*. This assemblage also contains some Cretaceous and Paleogene reworking. Low sample resolution in this hole due to very low recovery makes it difficult to solve age discrepancies between calcareous nannofossils and planktonic foraminifera. Additionally, the stratigraphy of sediments in the area of TDP Site 25 might be disrupted by thrust fault systems (e.g., thrust duplex in Miocene clays close to Ras Bura) (see Fig. 8 in Nicholas et al., 2007), which complicates accurate age assignments.

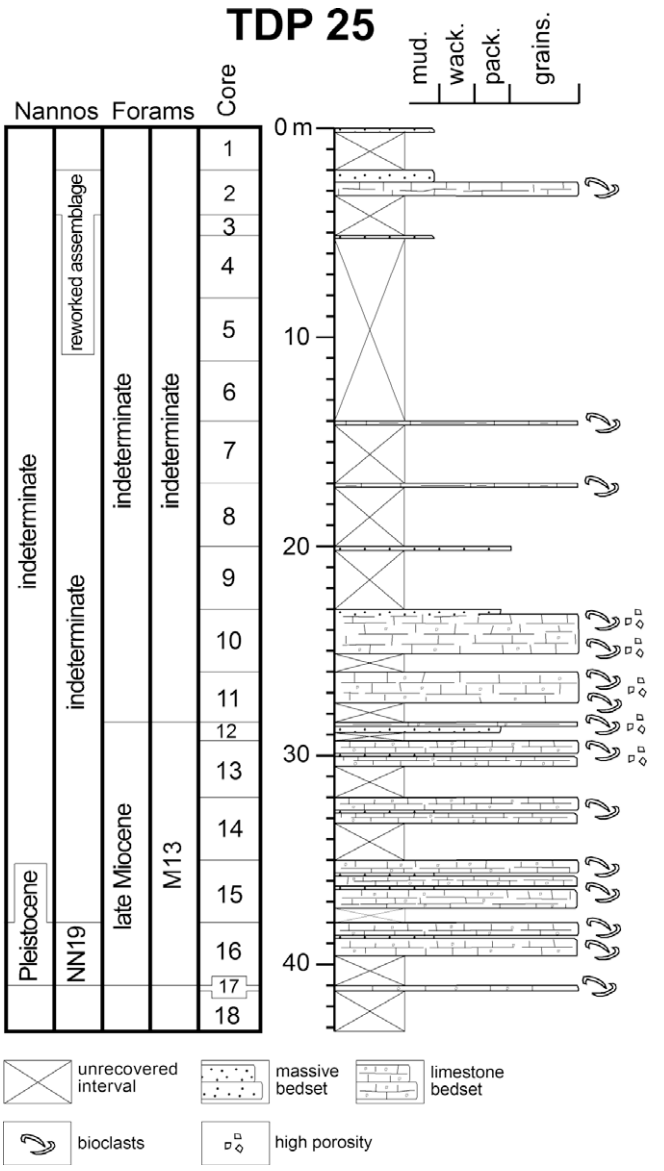

Fig. 10. Integrated lithostratigraphy, planktonic foraminiferal and calcareous nannofossil biostratigraphy of TDP Site 25.

Table 8
Cored intervals in TDP Site 25.

Site	Core	Top (m)	Bottom (m)	Drilled (m)	Recovered (m)	Recovery (%)
TDP25/	1	0.00	2.00	2.00	0.15	7.50
	2	2.00	4.10	2.10	1.20	57.14
	3	4.10	5.10	1.00	0.00	0.00
	4	5.10	8.10	3.00	0.10	3.33
	5	8.10	11.10	3.00	0.00	0.00
	6	11.10	14.00	2.90	0.00	0.00
	7	14.00	17.00	3.00	0.08	2.67
	8	17.00	20.00	3.00	0.10	3.33
	9	20.00	23.00	3.00	0.04	1.33
	10	23.00	26.00	3.00	2.10	70.00
	11	26.00	28.40	2.40	1.48	61.67
	12	28.40	29.30	0.90	0.56	62.22
	13	29.30	32.00	2.70	2.27	84.07
	14	32.00	35.00	3.00	1.20	40.00
	15	35.00	38.00	3.00	2.28	76.00
	16	38.00	41.00	3.00	1.63	54.33
	17	41.00	41.20	0.20	0.13	65.00
	18	41.20	43.20	2.00	0.05	2.50
	Total drilled: 43.20 m			Total recovered: 13.37 m		Recovery: 30.95%

4.7. TDP Site 26

TDP Site 26 was drilled 0.26 km to the NE of TDP Site 24, at a mid distance along the track between TDP Site 21 and the main road to Lindi (UTM 35L 570719, 8891946) (Figs. 2 and 3). The goal was to drill lower Turonian–middle Cenomanian sediments and try to completely recover the C–T boundary interval partially found in the upper portions of the nearby TDP Site 24 and 24B. The site was drilled to 56.17 m, with good recovery from 10.90 m to the bottom of the hole, and moderate recovery from the surface to 10.90 m (Table 9). Drilling was terminated the last day of the 2007 field season, once it was confirmed that middle Cenomanian sediments had been cored.

4.7.1. Lithostratigraphy

The principal lithologies from the surface to 16.90 m are light gray, massive, sandy siltstones with interbeds of cm- to dm-thick, grayish orange, lithified, medium- to coarse-grained sandstones with no macrofossil content (Figs. 5f, 11). From 16.90 m to the bottom of the hole, the dominant lithologies are medium light gray, massive siltstones that become more cemented and lithified in parts. No bioturbation is observed in this interval and fossil occurrences are limited to sporadic shell bioclasts.

4.7.2. Planktonic foraminiferal biostratigraphy

Planktonic foraminiferal assemblages at TDP Site 26 enable recognition of the *W. archaeocretacea* Zone (early Turonian) in core TDP26/1 to the uppermost part of 6 (the upper 8.03 m of the section) (Fig. 11, Table 1). An unconformity placed at 8.03 m separates the overlying *W. archaeocretacea* Zone from the underlying lower part of the *R. cushmani* Zone (middle-late Cenomanian), which is identified in core TDP26/6 to the bottom of the hole. As in TDP Site 24, samples studied in this site generally yield well preserved foraminifera, with occasional specimens exhibiting glassy shells that lack internal calcite or sediment infilling.

4.7.3. Calcareous nannofossil biostratigraphy

Nannofossil preservation is generally good throughout this site. Core TDP26/1 through the uppermost part of two lies in the early to middle Turonian subzone UC8a, which is underlain by the early Turonian UC6a–7 (Fig. 11, Table 2). The latter interval (core TDP26/2–6) coincides with highest values of the organic $\delta^{13}C$ profile due to OAE2 (see below), as observed at other sites. Then, a condensed interval in cores TDP26/6–7, with nannofossil assemblages of UC3c–UC5c, is assigned to the late Cenomanian–earliest Turonian. Below this unit, a relatively expanded succession of middle to late Cenomanian age (UC3a–b), as seen in TDP Sites 24 and 24B, is detected. The bottom of the hole is assigned to the early Cenomanian subzones UC1a–2c.

4.7.4. Chemostratigraphy

The bulk organic $\delta^{13}C$ ranges from −18.94‰ to −25.38‰ (average = −22.85‰ ± 2.01‰), and the curve exhibits low variability from the bottom of the section to 17.47 m (Fig. 10). From this point to 2.14 m, a remarkable, positive excursion with two peaks (5.80‰ total shift) is observed and assigned to part of the isotopic change due to OAE2. Then, the curve finishes with a 2.34‰ negative change in the uppermost sample. A correlation of TDP Site 26 with 24 and 24B and 21, based on the organic $\delta^{13}C$, shows that the former section is more expanded below and within the interval assigned to part of OAE2 (Fig. 12). Further, this correlation, together with the generally good microfossil preservation, suggests that the four sections have great potential to examine foraminiferal isotopic temperatures across OAE2 in Tanzania. The bulk carbonate isotopic records of TDP Site 26, though, do not show similar excursions (Fig. 12). Instead, the $\delta^{13}C$ and $\delta^{18}O$ curves present relatively low variability, with the exception of four samples with extremely low $\delta^{13}C$ at the bottom and top of the section. The $\delta^{13}C$ ranges from −0.24‰ to −11.67‰ (average = −2.64‰ ± 3.16‰) and the $\delta^{18}O$ ranges from −3.55‰ to −5.53‰ (average = −4.31‰ ± 0.66‰).

5. Lithofacies and sedimentary conditions

The lithostratigraphy of the drilled sites reveals vertical successions of varying lithologies that can be grouped into five different lithofacies (Table 10), according to variations in texture, grain size, color and depositional structures. The inferred lithofacies and the interpretation of the sedimentary conditions are below:

Lithofacies 1 occurs in TDP Sites 21 (Fig. 4) and 24 (Fig. 8), and is characterized by cm- to dm-thick, light gray, medium- to coarse-grained sandstones (~60% of the facies) and irregular

Table 9
Cored intervals in TDP Site 26.

Site	Core	Top (m)	Bottom (m)	Drilled (m)	Recovered (m)	Recovery (%)
TDP26/	1	0.00	1.90	1.90	0.92	48
	2	1.90	3.30	1.40	0.98	70
	3	3.30	4.90	1.60	0.17	11
	4	4.90	6.50	1.60	0.60	38
	5	6.50	7.90	1.40	0.84	60
	6	7.90	10.90	3.00	0.94	31
	7	10.90	14.03	3.13	3.13	100
	8	14.03	16.90	2.87	2.41	84
	9	16.90	19.90	3.00	1.40	47
	10	19.90	22.90	3.00	1.40	47
	11	22.90	25.90	3.00	2.87	96
	12	25.90	29.10	3.20	3.20	100
	13	29.10	32.00	2.90	2.59	89
	14	32.00	35.00	3.00	2.91	97
	15	35.00	38.00	3.00	2.86	95
	16	38.00	41.00	3.00	2.49	83
	17	41.00	44.00	3.00	2.98	99
	18	44.00	47.17	3.17	3.17	100
	19	47.17	50.00	2.83	2.83	100
	20	50.00	53.00	3.00	2.72	91
	21	53.00	56.17	3.17	3.17	100
	Total drilled: 56.17 m			Total recovered: 44.58 m		Recovery: 79.37%

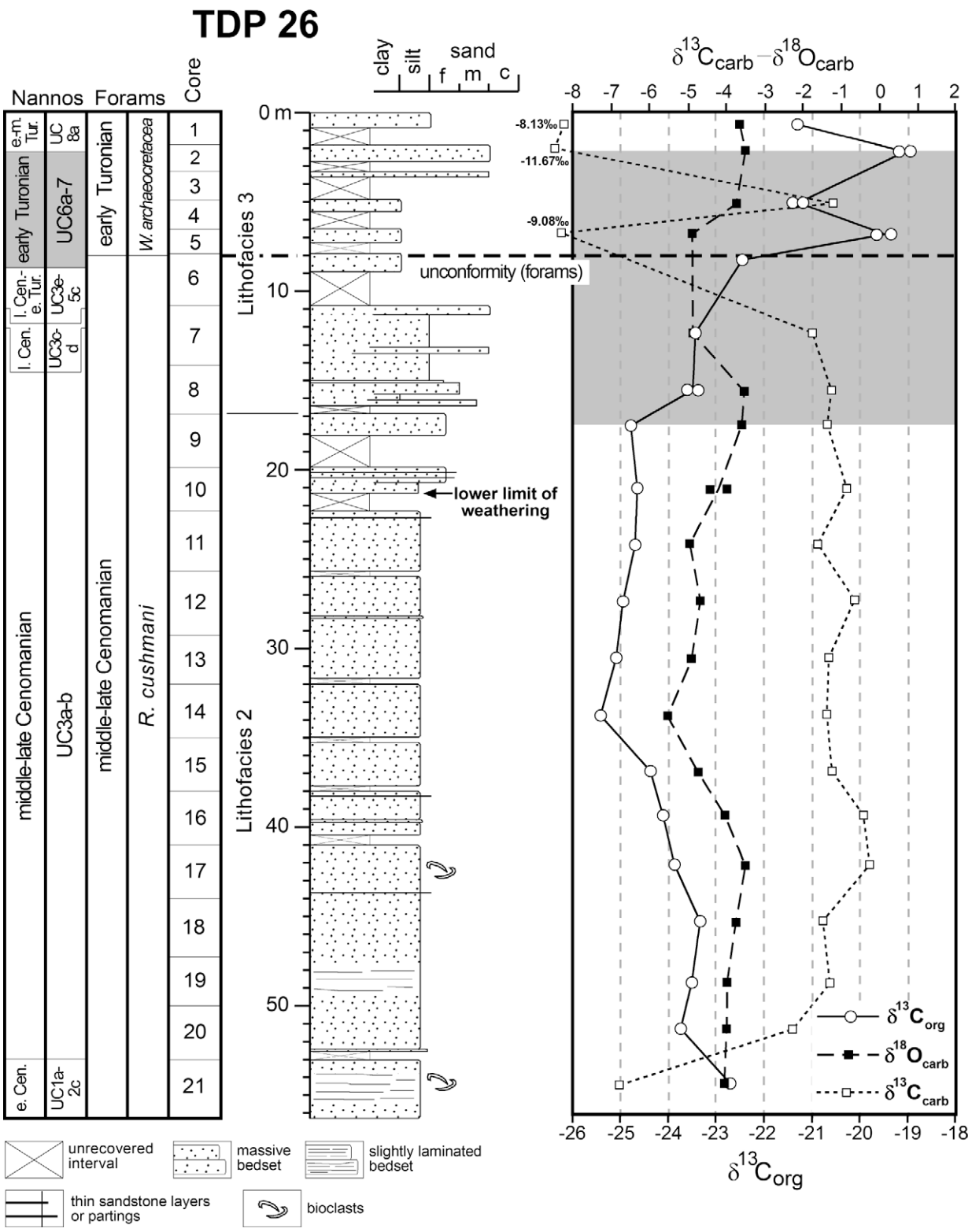

Fig. 11. Integrated lithostratigraphy, planktonic foraminiferal and calcareous nannofossil biostratigraphy, and chemostratigraphy of TDP Site 26. Lower limit of weathering in core 10 indicated. The gray shadow on the isotopic curves as in Fig. 4; e.-m. Tur.: early-middle Turonian; l. Cen.–e. Tur.: late Cenomanian–earliest Turonian; e. Cen.: early Cenomanian.

intercalations of cm-thick, grayish olive green, sandy siltstones (Fig. 5a and b, Table 10). The coarse-grained sandstone beds are typically massive and sharp-based. Some of the thickest sandstones have polymictic conglomeratic bases and normal gradation. In other instances, lamination at the top is visible. Further, greenish soft siltstone clasts and woody debris are found in the sandstones, and small bioturbation mottling is present in the siltstones.

The dominance of massive, coarse-grained sandstone layers with sharp, irregular basal contacts, together with occasional conglomeratic bases, suggests sedimentation by short-lived,

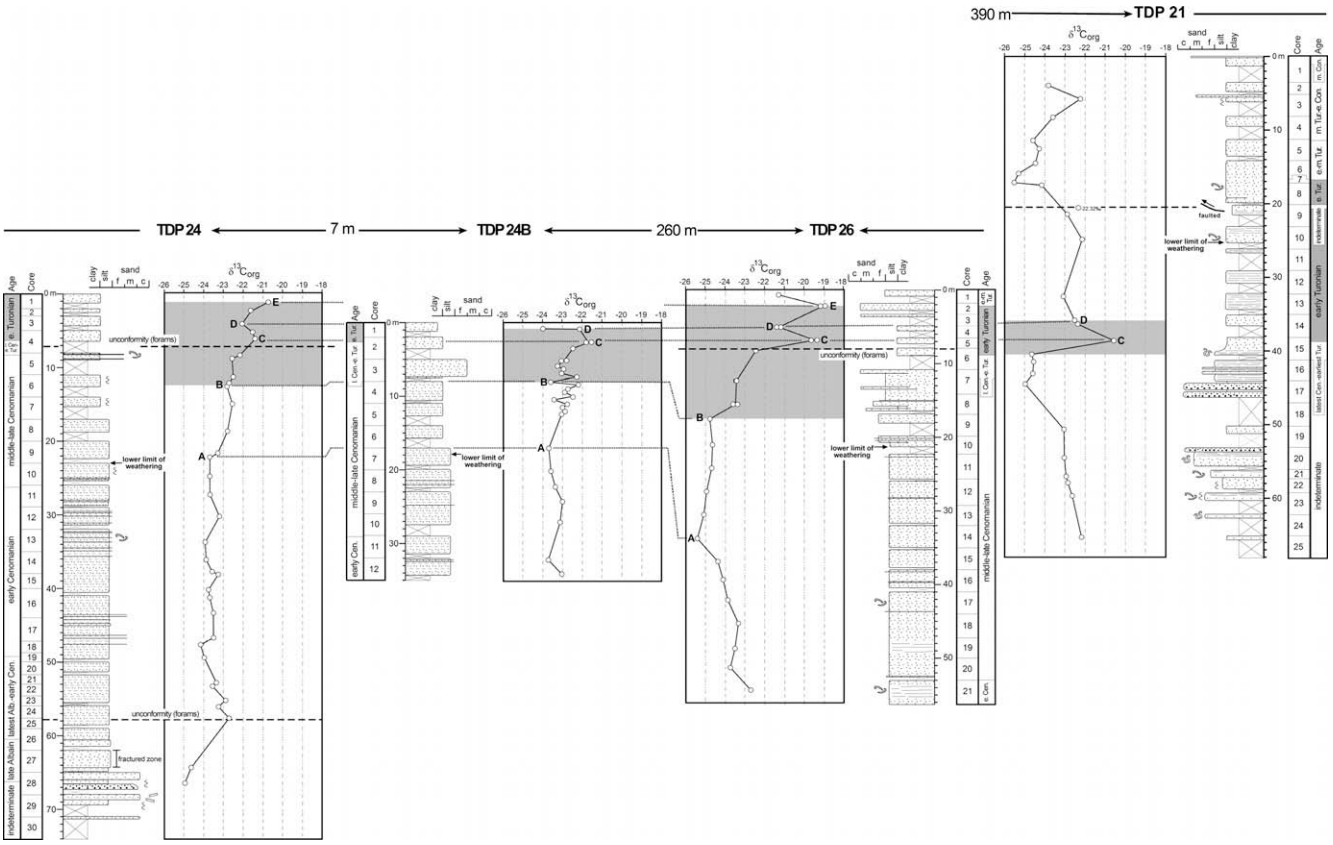

Fig. 12. Correlation of TDP Sites 21, 24, 24B and 26, based on the organic $\delta^{13}C$ stratigraphy. The gray shadow on the isotopic curves as in Fig. 4. Up to five tie-points (A–E) are interpreted along the isotopic profiles and used to correlate the sections. Ages are based on the calcareous nannofossil biozones. For explanations of age abbreviations, see captions of Figs. 4, 8, 9 and 11.

Table 10
Summary of characteristics of lithofacies 1–5, as identified in TDP Sites 21–26. Age assignment for distinct lithofacies can be seen in the lithostratigraphic log of each site.

Lithofacies	Occurrence	Characteristics	Interpretation/remarks
1	From 39.97 m to 68.10 m in TDP21; from 65 m to 75 m in TDP24	cm- to dm-thick, light gray, medium to coarse sandstones with sporadic woody debris, and cm intercalations of sandy siltstones; conglomeratic bases, normal gradation and lamination at the top are occasional in the sandstones	Upper slope, but not too far from the shoreline
2	From 11 m to 65 m in TDP24; from 8 m to 35 m in TDP24B; from 19.60 m to 56.17 m in TDP26; entire TDP22 section	Dark, mm to cm-thick interbeds of siltstones and fine sandstones; presence of organic-rich laminated intervals; abundant soft-sediment deformation in TDP22; sporadic ammonite and inoceramid debris throughout	Outer shelf below the storm wave base; low levels of benthic oxygenation
3	From 0 m to 8.10 m in TDP21; from 0 m to 11 m in TDP24; from 0 m to 8 m in TDP24B; from 0 m to 16.90 m in TDP26	dm to m thick, massive claystones and siltstones, with cm intercalations of brownish gray, lithified, massive, medium to coarse sandstones	Upper slope; relatively low energy
4	Form 8.10 m to 39.97 m in TDP21	Bluish gray, massive claystones to silty claystones	Shelf below the storm wave base; low-energy conditions
5	Entire TDP23 section	dm to m thick, bluish gray claystones and greenish gray, sandy siltstones, with thin layers of fine sandstones; bioturbation burrows frequent at some intervals; ammonite and inoceramid debris present	Outer shelf below the storm wave base; normal levels of benthic oxygenation and nutrient content

high-energy events that could have originated from turbulent flows (Browne et al., 2000; Wach et al., 2000). Some of these flows transported up to gravel-size detritus and possibly ripped up soft clasts from the semi-lithified seafloor. The presence of normal gradation and laminated top intervals in some sandstone beds are interpreted as reflecting a progressive energy decrease in the turbulent flow as it diluted along its path. Together, these characteristics suggest deposition in an upper slope environment, although the shoreline could not have been too far away as inferred from the woody debris in the sandstones. The siltstone intervals correspond to periods of lower energy, when fine detritus, brought in suspension probably by surface- to mid-water flows, settled. Bioturbation mottling in the siltstones indicates hospitable benthic waters for burrowing fauna during the low energy periods.

Lithofacies 2 occurs in TDP Sites 24 (Fig. 8), 24B (Fig. 9), 26 (Fig. 11), and through the entire section of TDP Site 22 (Fig. 6). The dominant lithologies are mm- to cm-thick interbeds of rarely bioturbated, dark gray siltstones and fine-grained sandstones (Fig. 5c and d, Table 10) (~95% of the facies) with limited presence of light, fine-grained sandstone partings. Contacts between the interbeds are normally gradational, although some sandstones

display sharp basal contacts. Laminated, organic-rich intervals are common throughout TDP Site 22. Soft-sediment deformation is abundant at TDP Site 22, but absent from TDP Sites 24, 24B and 26. Disseminated pyrite is locally present and macrofossils observed include ammonite and inoceramid debris, along with undetermined bioclasts.

The abundance of silt and fine sand, together with the existence of ammonite and inoceramid remains, indicates fully-open marine conditions, and the predominant absence of depositional structures points to sedimentation below the storm wave base in an outer shelf environment. Because some of the fine-grained sandstone interbeds in this lithofacies are sharp-based, bottom currents could have episodically transported fine sand offshore. Further, the light sandstone partings may be interpreted as reflecting pulses of small bottom currents that introduced fine sand from shallower sites (Pearson et al., 2004, 2006). Yet, the dominant depositional mechanism was probably surface- to mid-water flows that held silt and fine sand in suspension until dilution of the flow allowed the sediment to settle. Finally, the scarcity of bioturbation and the presence of fine lamination may indicate relative oxygen depletion in bottom waters that prevented prolonged habitation by burrowing organisms (Henderson et al., 2004; Jiménez Berrocoso et al., 2008).

Lithofacies 3 is present in TDP Sites 21 (Fig. 4), 24 (Fig. 8), 24B (Fig. 9) and 26 (Fig. 11), and characterized by dm- to m-thick intervals of massive claystones and siltstones (50–95% of the facies) with cm-thick intercalations of brownish gray, lithified, massive, medium- to coarse-grained sandstones (up to 50% of the facies) (Fig. 5e and f, Table 10). A thin sandstone layer, with an accumulation of shell fragments in the middle and wavy lamination at the top, is also observed at TDP Site 24. No other fossil occurrences are found and bioturbation mottling is only rarely visible in the siltstones of TDP Site 21.

The existence of cm-thick layers of medium- to coarse-grained sandstones indicates that bottom currents were relatively common and transported medium and coarse sand to the depositional area during high-energy episodes (e.g., Pattison, 2005). Indeed, small shells accumulated in the middle of a sandstone layer with surface lamination indicate that turbulent flows could develop during formation of this lithofacies. These characteristics suggest an upper slope environment for lithofacies 3. The dominance of silt and clay detritus, however, indicates that low-energy conditions prevailed for long periods and particle settling was the main background depositional mechanism. On the other hand, an unconformity is interpreted from the foraminiferal biostratigraphy close to the C–T transition in lithofacies 3 of TDP Sites 24 and 26 (Figs. 8, 11 and 12), whereas condensation of the stratigraphic record is deduced from the nannofossil biostratigraphy across the same interval of these sites, including TDP Site 24B (Fig. 9). This situation suggests that fluctuations in the sedimentation rate may have occurred around the C–T transition in these sections, although higher-resolution biostratigraphy is required to accurately constrain this scenario.

Lithofacies 4 occurs in TDP Site 21 (Fig. 4) and comprises bluish gray, massive claystones to silty claystones (Fig. 5g and h, Table 10). Some intervals present faint horizontal lamination. Bioturbation is not visible and fossils are limited to scarce bioclast debris.

The absence of depositional structures suggests that sedimentation of lithofacies 4 took place under very low-energy conditions in a shelf environment below the storm wave base. The high percentage of planktonic foraminifera in the samples studied from this lithofacies, though, suggests deposition near or below the shelf break. The dominant depositional mechanism was possibly settling of very fine detritus.

Lithofacies 5 represents the entire stratigraphic interval of TDP Site 23 (Fig. 7). It consists of dm- to m-thick, massive, bluish gray, calcareous claystones to siltstones and greenish gray, sandy siltstones (~95% of the facies) (Fig. 5i and j, Table 10). Thin layers of light gray, fine-grained sandstones are also present. These layers are massive and typically have sharp irregular basal contacts (Fig. 5i). Macrofossil occurrences include ammonite and inoceramid debris, in addition to undifferentiated bioclasts. The presence of mm- to cm-size, bedding-parallel or vertical bioturbation burrows is frequent at some intervals (Fig. 5j).

The dominance of clay-sized grains and the existence of ammonite and inoceramid remains are evidence of deposition on the outer shelf under low-energy conditions, where the main sedimentation mechanism was likely fine particle settling. This environment was below the storm wave base level, but it probably experienced moderately frequent bottom-current pulses that brought fine sand offshore, as inferred from the thin, light, fine-grained sandstones (Pearson et al., 2004, 2006). The common existence of bioturbation burrows at some intervals indicates periods of favorable oxygen levels and nutrient concentrations in benthic waters for burrowing fauna.

6. Concluding remarks

The TDP expedition in 2007 targeted the Upper Cretaceous sequence of the Lindi area in southern Tanzania, where previous TDP drilling had only recovered thin, discontinuous Albian–Maastrichtian successions and mapped Campanian–Oligocene sediments. In 2007, six new Upper Cretaceous sites (TDP Site 21, 22, 23, 24, 24B and 26) and a thin Miocene–Pleistocene section (TDP Site 25) were cored, and a significant area to the S and SW of Kitulo Hill was explored and mapped. The geological map of the region has been revised herein, based on the 2007 information. Together, all the data indicate a much more expanded and complete Upper Cretaceous marine sequence than previously recognized in southern Tanzania.

Main lithologies of the new sites include thick intervals of dark claystones and siltstones, containing organic-rich laminated parts, irregular silty to fine sandstone partings, and rare inoceramid and ammonite debris. Minor lithologies consist of much thinner intervals of gray, medium to coarse sandstones with occasional conglomeratic bases and sporadic woody debris. These lithologies have been grouped into five distinct lithofacies and some of them are identified more than once in the total stratigraphic interval drilled. The lithofacies analysis suggests that the depositional environment could fluctuate between outer shelf and upper slope, although the shoreline was possibly not too far from the sedimentation site, especially during deposition of the coarse sandstone intervals as inferred from the presence of woody debris. These inferences suggest that, during most of the Late Cretaceous, the Tanzanian margin largely experienced the deposition of typical shelf facies. Further, this situation indicates that microfossils collected from these sediments have great potential to provide open ocean temperatures from a stable continental margin environment of the subtropical Late Cretaceous.

The planktonic foraminiferal assemblages are extraordinarily well preserved through the Turonian intervals cored and in some of the most clay-rich units of the Cenomanian and Campanian. The remaining intervals generally yield moderately to well preserved foraminifera. The assemblages are moderately diverse and include key zonal marker taxa that can be used to reliably correlate with the standard Tethyan biozonation of Robaszynski and Caron (1995). Foraminiferal biostratigraphic results indicate that (1) TDP Sites 24, 24B and 26 together span the latest Albian–early Turonian (*P. buxtorfi* to *W. archaeocretacea* Zones), (2) TDP Site 21 and 22 collectively record an expanded sequence of the earliest Turonian–Coniacian (*W. archaeocretacea–D. concavata* Zones), including a thin early Eocene (E4 Zone) faulted slice within TDP

Site 21, (3) TDP Site 23 records a thick section of the early to late Campanian (*G. ventricosa–R. calcarata* Zones), and (4) TDP Site 25 represents a thin section of the Miocene (M13 Zone).

The nannofloras are similarly very well preserved, with taxa typically having the lowest preservation potential (e.g., holococcoliths and small, delicate heterococcoliths) being continuously preserved. The excellent nannofossil preservation through the interval ascribed to UC3c–7 (late Cenomanian–early Turonian), correlating with an organic $\delta^{13}C$ positive excursion due to OAE2, will allow us to examine changes in biodiversity at this time, when increased extinctions and inceptions of taxa have been postulated. Additionally, this situation will be used to test hypotheses of surface-water fertility and its effect on nannofossil abundance patterns. On the other hand, the apparent absence of some of the subzonal markers of the UC biozonation scheme may provide insights into biogeographic constraints on these maker taxa, as opposed to preservational biases. Even more significantly, it will be possible to accurately calibrate the preservationally-unbiased nannofossil and planktonic foraminiferal zonations and adjust the interpreted ages, which, as can be seen from the figures herein, are sometimes out of synchronization.

The chemostratigraphic record of the sites reveals (1) largely invariable bulk organic $\delta^{13}C$ profiles, and (2) a positive excursion of up to 5.80‰ that correlates across TDP Sites 21, 24, 24B and 26, and suggests recovery of part of OAE2. The bulk carbonate $\delta^{13}C$ and $\delta^{18}O$ profiles generally show higher variability, which is interpreted as reflecting minor alteration by secondary carbonate cementation, even though foraminifera and nannofossils are often very well preserved. Shifts to markedly low values in the $\delta^{13}C$ and $\delta^{18}O$ indicate alteration attributable to deep weathering under the modern Tanzanian tropical conditions and/or incorporation of remineralized organic carbon. Our isotopic profiles represent the first chemostratigraphy reported for upper Albian–upper Campanian marine sediments in Tanzania and, together with the litho- and biostratigraphy of the new sites, outline the stratigraphic context for forthcoming results that will test models of climate dynamics and ice-sheet growth during the Late Cretaceous greenhouse world.

Acknowledgments

The Tanzania Petroleum Development Corporation is gratefully acknowledged for logistical support, and the Tanzania Commission for Science and Technology is thanked for permission to carry out this research in the field. We greatly appreciate the generous hospitality and valuable technical assistance of Ephrem Mchana, Michael Mkereme and Elvis Mgaya (Mr. K). S.W. Lepley and C.A. Kelley are acknowledged for assistance with the isotopic analysis, and C.J. Nicholas and P.N. Pearson for constructive comments on the manuscript. P. Eriksson is thanked for editorial handling. Field work and drilling were funded by a USA National Science Foundation grant to KGM and BTH (EAR 0642993). Participation of JAL was funded by a Natural Environmental Research Council Grant (NE/C510508/1) and the UCL Graduate School. PRB was partly funded by the UCL Graduate School.

References

Balduzzi, A., Msaky, E., Trincianti, E., Manum, S.B., 1992. Mesozoic Karoo and post-Karoo formations in the Kilwa area, southeastern Tanzania – a stratigraphic study based on palynology, micropalaeontology and well log data from the Kizimbani Well. Journal of African Earth Sciences 15, 405–427.

Benitah-Lipson, S., 2008. Phylogeny of the middle Cretaceous (late Albian–late Cenomanian) planktonic foraminiferal general *Parathalmanninella* nov. Gen. and *Thalmanninella*. Journal of Foraminiferal Research 38, 183–189.

Berggren, W.A., Pearson, P.N., 2005. A revised tropical to subtropical Paleogene planktonic foraminiferal zonation. Journal of Foraminiferal Research 35, 279–298.

Bown, P.R., 2005. Palaeogene calcareous nannofossils from the Kilwa and Lindi areas of coastal Tanzania (Tanzania drilling project 2003–2004). Journal of Nannoplankton Research 27, 21–95.

Bown, P.R., Young, J.R., 1998. Techniques. In: Bown, P.R. (Ed.), Calcareous Nannofossil Biostratigraphy, British Micropalaeontological Society Series. Chapman and Hall/Kluwer Academic Press, pp. 16–28.

Bown, P.R., Dunkley Jones, T., 2006. New Palaeogene calcareous nannofossil taxa from coastal Tanzania: Tanzania drilling project sites 11–14. Journal of Nannoplankton Research, 28.

Browne, G.H., Slatt, R.M., King, P.R., 2000. Contrasting styles of basin-floor fan and slope fan deposition: Mount Messenger Formation, New Zealand. In: Bouma, A.H., Stone, C.G., (Eds.), Fine-grained turbidite systems, AAPG Memoir 72/SEPM (Society for Sedimentary geology), Special publication 68, pp. 143–152.

Burnett, J.A. (with contributions from Gallagher, L.T. and Hampton, M.J.), 1998. Upper Cretaceous. In: Bown, P.R. (Ed.), Calcareous Nannofossil Biostratigraphy. British Micropalaeontological Society Series, Chapman and Hall/Kluwer Academic Press, pp. 132–199.

Ernst, G., Schlüter, T., 1989. The Upper Cretaceous of the Kilwa Region, coastal Tanzania. In: Workshop Geol. Tanzania Rev. Res. Progr. University of Köln, Abstr., Cologne, pp. 1–3.

Ernst, G., Zander, J., 1993. Stratigraphy, facies development, and trace fossils of the Upper Cretaceous of southern Tanzania (Kilwa District). In: Geology and Mineral resources of Somalia and surrounding areas, Inst. Agron. Oltremare Firenze, Relaz. E Monogr.113, Firenze, pp. 259–278.

Gierlowski-Kordesch, E., Ernst, G., 1987. A flysch trace assemblage from the Upper Cretaceous shelf of Tanzania. In: Matheis, G., Schandelmeier, H. (Eds.). Current Research in African Earth Sciences, pp. 217–222.

Handley, L., Pearson, P.N., McMillan, I.K., Pancost, R.D., 2008. Large terrestrial and marine carbon and hydrogen isotope excursion in a new Paleocene/Eocene boundary section from Tanzania. Earth and Planetary Science Letters 275, 17–25.

Henderson, R.A., 2004. A mid-Cretaceous association of shell beds and organic-rich shale: bivalve exploitation of a nutrient-rich, anoxic sea-floor environment. Palaios 19, 156–169.

Huber, B.T., MacLeod, K.G., Tur, N.A., 2008. Chronostratigraphic framework for upper Campanian–Maastrichtian sediments on the blake nose (subtropical North Atlantic). Journal of Foraminiferal Research 38, 162–182.

Jenkyns, H.C., 1980. Cretaceous anoxic events: from continents to oceans. Journal of the Geological Society 137, 171–188.

Jiménez Berrocoso, A., MacLeod, K.G., Calvert, S.E., Elorza, J., 2008. Bottom water anoxia, inoceramid colonization, and bentho-pelagic coupling during black shale deposition on Demerara Rise (Late Cretaceous western tropical North Atlantic). Paleoceanography 23, PA3212.

Kent, P.E., Hunt, J.A., Johnstone, D.W., 1971. The Geology and Geophysics of Coastal Tanzania. Institute of Geological Sciences Geophysical Paper No.6, i-vi, 1-101.HMSO, London.

Key, R.M., Smith, R.A., Smelor, M., Sæther, O.M., Thorsnes, T., Powell, J.H., Njange, F., Zandamela, E.B., 2008. Revised lithostratigraphy of the Mesozoic–Cenozoic succession of the onshore Rovuma Basin, northern coastal Mozambique. South African Journal of Geology 111, 89–108.

Lees, J.A., 2007. New and rarely reported calcareous nannofossils from the Late Cretaceous of coastal Tanzania: outcrop samples and Tanzania drilling project sites 5, 9 and 15. Journal of Nannoplankton Research 29, 39–65.

Martini, E. 1971. Standard Tertiary and Quaternary calcareous nannoplankton zonation. In: Farinacci, A. (Ed.), Proceedings II Planktonic Conference, Roma 1970. Edizioni Tecnoscienza, Rome 2, pp. 739–785.

Moore, W.R., McBeath, D.M., Linton, R.E., Terris, A.P., Stoneley, R., 1963. Geological Survey of Tanganyika Quarter Degree Sheet 256 and 256E. 1:125 000 Kilwa, first ed. Geological Survey Division, Dodoma.

Mpanda, S., 1997. Geological development of the East African coastal basin of Tanzania. Stockholm Contributions in Geology, vol 45. University of Stockholm, Sweden, pp. 1–121.

Nicholas, C.J., Pearson, P.N., Bown, P.R., Dunkley Jones, T., Huber, B.T., Karega, A., Lees, J.A., McMillan, I.K., O'Halloran, A., Singano, J., Wade, B.S., 2006. Stratigraphy and sedimentology of the upper Cretaceous to Paleogene Kilwa Group, southern coastal Tanzania. Journal of African Earth Sciences 45, 431–466.

Nicholas, C.J., Pearson, P.N., McMillan, I.K., Ditchfield, P.W., Singano, J.S., 2007. Structural evolution of coastal Tanzania since the Jurassic. Journal of African Earth Sciences 48, 273–297.

Ogg, J.G., Agterberg, F.P., Gradstein, F.M., 2004. The Cretaceous period. In: Gradstein, F.M., Ogg, J.G., Smith, A.G. (Eds.), A Geologic Time Scale. Cambridge University Press, Cambridge, pp. 344–383.

Pattison, S.A.J., 2005. Storm-influenced prodelta turbidite complex in the Lower Kenilworth Member at Hatch Mesa, Book Cliffs, Utah. USA: implications for shallow marine facies model. Journal of Sedimentary Research 75, 420–439.

Pearson, P.N., Ditchfield, P.W., Singano, J., Harcourt-Brown, K.G., Nicholas, C.J., Olsson, R.K., Shackleton, N.J., Hall, M.A., 2001. Warm tropical sea surface temperatures in the Late Cretaceous and Eocene epochs. Nature 413, 481–487.

Pearson, P.N., Nicholas, C.J., Singano, J.M., Bown, P.R., Coxall, H.K., van Dongen, B.E., Huber, B.T., Karega, A., Lees, J.A., Msaky, E., Pancost, R.D., Pearson, M., Roberts, A.P., 2004. Paleogene and Cretaceous sediment cores from the Kilwa and Lindi areas of coastal Tanzania: Tanzania drilling project sites 1–5. Journal of African Earth Sciences 39, 25–62.

Pearson, P.N., Nicholas, C.J., Singano, J.M., Bown, P.R., Coxall, H.K., van Dongen, B.E., Huber, B.T., Karega, A., Lees, J.A., MacLeod, K., McMillan, I.K., Pancost, R.D., Pearson, M., Msaky, E., 2006. Further Paleogene and Cretaceous sediment cores from the Kilwa area of coastal Tanzania: Tanzania drilling project sites 6–10. Journal of African Earth Sciences 45, 279–317.

Pearson, P.N., van Dongen, B.E., Nicholas, C.J., Pancost, R.D., Schouten, S., Singano, J.M., Wade, B.S., 2007. Stable warm tropical climate through the Eocene Epoch. Geology 35, 211–214.

Pearson, P.N., McMillan, I.K., Singano, J.M., Wade, B.S., Jones, T.D., Coxall, H.K., Bown, P.R., Lear, C.H., 2008. Extinction and environmental change across the Eocene–Oligocene boundary in Tanzania. Geology 36, 179–182.

Robaszynski, F., Caron, M., 1995. Foraminifères planktoniques du Crétacé: commentaire de la zonation Europe-Méditerranée. Société géologique de France 166, 681–692.

Salman, G., Abdula, I., 1995. Development of the Mozambique and Ruvuma sedimentary basins, offshore Mozambique. Sedimentary Geology 96, 7–41.

Schlanger, S.O., Jenkyns, H.C., 1976. Cretaceous oceanic anoxic events: causes and consequences. Geologie en Mijnbouw 55, 179–184.

Schlüter, T., 1997. Geology of East Africa. Borntraeger, Stuttgart. 512 p.

Schlüter, T., 2008. Geological Atlas of Africa: With Notes on Stratigraphy, Tectonics, Economic Geology, Geohazards, Geosites and Geoscientific Education of Each Country. Springer. 308 p.

Stewart, D.R.M., Pearson, P.N., Ditchfield, P.W., Singano, J.M., 2004. Miocene tropical Indian Ocean temperatures: evidence from three exceptionally preserved foraminiferal assemblages in Tanzania. Journal of African Earth Sciences 40, 173–190.

Wach, G.D., Lukas, T.C., Goldhammer, R.K., Wickens, H.D., Bouma, A.H., 2000. Submarine fan through slope to deltaic transition basin-fill succession, Tanqua Karoo, South Africa. In: Bouma, A.H., Stone, C.G. (Eds.), Fine-grained turbidite systems, AAPG Memoir 72/SEPM (Society for Sedimentary Geology), Special publication 68, pp. 173–180.